Biophysical Reports

REVIEW

A review of TNP-ATP in protein binding studies: benefits and pitfalls

Dixon J. Woodbury,[1,2,*] Emily Campbell Whitt,[1] and Robert E. Coffman[2]
[1]Department of Cell Biology and Physiology and [2]Neuroscience Center, Brigham Young University, Provo, Utah

ABSTRACT We review 50 years of use of 2′,3′-O-trinitrophenyl (TNP)-ATP, a fluorescently tagged ATP analog. It has been extensively used to detect binding interactions of ATP to proteins and to measure parameters of those interactions such as the dissociation constant, K_d, or inhibitor dissociation constant, K_i. TNP-ATP has also found use in other applications, for example, as a fluorescence marker in microscopy, as a FRET pair, or as an antagonist (e.g., of P2X receptors). However, its use in protein binding studies has limitations because the TNP moiety often enhances binding affinity, and the fluorescence changes that occur with binding can be masked or mimicked in unexpected ways. The goal of this review is to provide a clear perspective of the pros and cons of using TNP-ATP to allow for better experimental design and less ambiguous data in future experiments using TNP-ATP and other TNP nucleotides.

WHY IT MATTERS 2′,3′-O-trinitrophenyl (TNP)-ATP is a fluorescent ATP analog used extensively for over 50 years to probe interactions of ATP with different proteins. However, the chemical features that render it useful may also confound interpretation of experiments measuring ATP binding. We review various experimental results achieved using TNP-ATP, as well as shedding light on potential pitfalls of its use. This will allow for better future planning and interpretation of experiments using TNP-ATP.

INTRODUCTION

ATP is a molecule that is essential in the function of all living things. It provides energy for reactions within cells and acts as a signal by binding to proteins and altering their function. 2′,3′-O-trinitrophenyl (TNP)-ATP is a fluorescently tagged ATP molecule that can be used to study how proteins interact with ATP. When TNP-ATP binds to proteins, the TNP fluorescence changes in intensity and peak wavelength, as does its absorbance spectra (difference spectra). These spectral changes are easier to measure than other methods for measuring ligand-protein interactions such as radioisotopes, x-ray crystallography, or circular dichroism.

Fig. 1 shows the structure of ATP and TNP-ATP along with its absorption and emission spectra. The fluorescent portion of the molecule has the IUPAC name of 2,4,6-trinitrophenol (TNP) and is derived from picric acid. TNP absorbs light at 408 and 470 nm and fluoresces at 561 nm in water. Changes in the environment of TNP-ATP such as changes in pH or entering the binding pocket of a protein alter its absorption and fluorescence spectra, making TNP-ATP a useful probe for ATP binding (Fig. 1). The TNP fluorophore, first synthesized in 1964 by Azegami and Iwai (1), is connected to the ribose sugar of the ATP molecule. The structure of TNP-ATP was confirmed by Hiratsuka via infrared spectral analysis and NMR in 1975 (2). The idea behind designing TNP-ATP is to have a fluorescent probe that interacts with proteins at their ATP binding sites and is still hydrolyzed by enzymes that hydrolyze ATP. If TNP-ATP is to mimic ATP's interaction with proteins that not only bind but also hydrolyze it, then TNP cannot be attached at one of ATP's three phosphate groups because they are critical for ATP's biological function as an energy molecule. Although these characteristics are useful, one problem is that the TNP moiety may also interact with proteins and change its binding affinity for

Submitted April 11, 2021, and accepted for publication August 3, 2021.

*Correspondence: dixon_woodbury@byu.edu

Emily Campbell Whitt's present address is Pathology and Laboratory Medicine, University of Rochester Medical Center, Rochester, New York 14642.

Editor: Andrey Klymchenko.

https://doi.org/10.1016/j.bpr.2021.100012

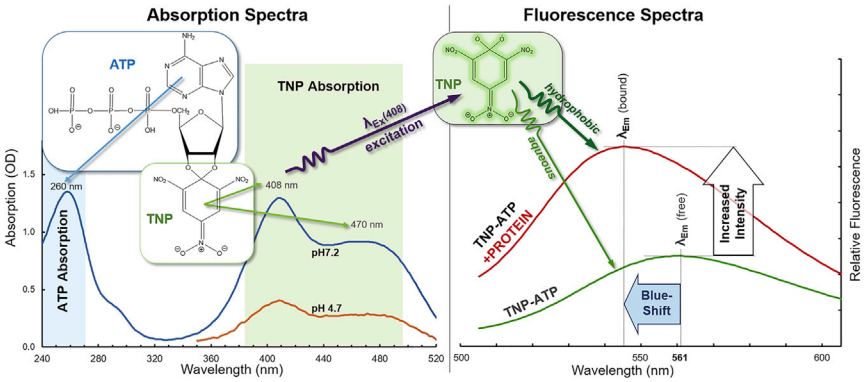

FIGURE 1 Absorption and fluorescence spectra of TNP-ATP. (*Left*) Absorption spectra of free TNP-ATP in 10 mM phosphate buffer at pH 7.2 (*blue*) and pH 4.7 (*orange*). Also shown is the structure of TNP-ATP, with ATP in the blue box and the fluorescent TNP moiety in the green box. ATP absorption peak occurs around 260 nm and is highlighted in blue. The TNP moiety has two absorption peaks at 408 and 470 nm, highlighted in green. TNP absorption increases with increasing pH. (*Right*) Fluorescence of free or bound TNP-ATP. The green box again shows the structure of the TNP moiety. When the TNP fluorophore is excited at $\lambda_{ex} = 408$ nm, as indicated by the purple arrow, it has an emission in water (*green line*) with a peak (λ_{em}) at 561 nm. When TNP-ATP binds to proteins, the fluorescence intensity increases and λ_{em} shifts to shorter wavelengths (blue shift) because of the hydrophobic environment in the protein binding site (*red solid line*). Competition by excess ATP should decrease intensity and red shift the peak to original values; however, complete reversal is seldom seen. In general, changes in TNP's fluorescence intensity and peak wavelength indicate its interactions with proteins.

proteins. Nevertheless, these characteristics make TNP-ATP a good probe to study ATP binding sites (3).

TNP-ATP's first reported use was in 1973 (4) to test whether it would interact with the meromyosin heavy-chain protein in a similar manner to its known interaction with ATP. In that study, Hiratsuka and Uchida demonstrated that TNP-ATP absorbance was sensitive to changes in pH, with absorbance increasing as pH increased (see Fig. 1, *left*). In 1975, Hiratsuka further demonstrated that increasing solvent polarity causes the wavelength of the absorption peak to increase (2). Other early studies also reported changes in TNP absorption spectra (sometimes in combination with fluorescent changes) when TNP-ATP bound to proteins (2–7). More recently, hundreds of works have used it in diverse ways, most commonly as a fluorescent probe in ligand binding studies. In the last 10 years, several step-by-step protocols for using TNP-ATP with protein kinases have been published (8,9), contributing to the usefulness of TNP-ATP.

This review will examine the fluorescent characteristics of TNP-ATP, how TNP-ATP has been used successfully in the past, and problems that have appeared in the literature with data obtained using TNP-ATP. Our goal is to provide a clear perspective of the pros and cons of using TNP-ATP and a list of best practices to allow for better experimental design and less ambiguous data in future studies.

Spectral characteristics of TNP-ATP

TNP-ATP is an excellent fluorescent probe because of its bright fluorescence, low quenching, and inherent sensitivity to the surrounding environment. In an aqueous solution at neutral pH, it has a single fluorescent emission maximum (λ_{em}) at 561 nm, but this emission increases severalfold in intensity and shifts to higher energies (blue shift, shorter wavelengths) when the molecule's environment changes, such as when TNP-ATP binds to a protein (3) (see Fig. 1). These properties are measured using a fluorimeter. The fluorimeter excites the TNP probe with light at a specific wavelength (λ_{ex}, typically at 408 nm) raising electrons to an excited (higher energy) state. When the electrons return to their resting state, they release the excess energy in the form of a photon. The fluorimeter measures the wavelength and number of photons emitted by TNP molecules in the sample.

An important aspect of TNP-ATP's usefulness as a probe, but also a concern, is that its absorption and emission spectra are highly sensitive to the surrounding environment. For example, as shown in Fig. 1 (*left*), acidic solutions cause the molecule to absorb less light and hence decrease fluorescent intensity (4,10–12). This is discussed further in Example 1: unexpected increase in fluorescence. Additionally, it has been shown that decreasing the polarity of the solvent in which TNP-ATP is dissolved (e.g., changing from H_2O to ethanol to dimethylformamide) causes an increase in the intensity and a decrease in λ_{em} (peak emission blue shift) of fluorescence by TNP-ATP (12,13), which looks the same as when TNP-ATP binds protein. Increasing the viscosity of the solvent has the same effect (12). Thus, TNP-ATP is highly sensitive to the pH, polarity, and viscosity of its surrounding environment, rendering it a useful molecule for sensing changes in environment as it enters the binding pocket of a protein. However, a secondary method to confirm ATP binding and ascertain the characteristics of that binding ensures proper interpretation of results.

In 1999, Ye et al. used time-resolved fluorescence spectroscopy to characterize how the environment changes TNP-ATP emission (11). They attribute fluorescence changes caused by solvent polarity to the

solvation effect, meaning that polar solvents are better able to stabilize the excited state of the TNP-ATP molecule, which causes a change in the emission spectrum. Likewise, they state that blue shifts in λ_{em} observed when TNP-ATP interacts with a protein's ATP binding site are "ascribed to the overlap of fluorescence spectra from free TNP-ATP and bound TNP-ATP." These effects allow researchers to use the fluorescence emission spectrum of TNP-ATP to infer how much TNP-ATP, and by extension ATP, is interacting with a given protein.

TNP-ATP has long been used, and continues to be used, to study how ATP interacts with individual proteins (3). TNP-ATP fluorescence is used in fluorescence microscopy to visualize the cellular location of proteins (14–18) and as a Förster or fluorescence resonance energy transfer (FRET) pair (19–26). Many physical properties of TNP-ATP, including absorption and fluorescence, have been previously reported and reviewed (3,13).

ATP binding studies using TNP-ATP

The characteristics of TNP-ATP outlined above have led to its broad use in studies of how proteins interact with and bind to ATP. Because of its shared characteristics with ATP, TNP-ATP has been used to establish whether ATP interacts with a specific protein and to attempt to understand the underlying kinetics of that binding.

Hiratsuka and Uchida's (4) original study on TNP-ATP used it to probe the ATP binding site of heavy-chain meromyosin. In this early experiment, the researchers used the absorption (not fluorescence) properties of TNP-ATP to find the dissociation constant, K_d, of TNP-ATP with heavy-chain meromyosin. This was done by adding increasing amounts of TNP-ATP to a fixed concentration of heavy-chain meromyosin and fitting the $\Delta A_{518\ nm}$ (difference absorbance at 518 nm) versus TNP-ATP alone to a theoretical curve. Since this time, there has been a shift away from using absorbance spectra to using fluorescence spectra, and many works have published the K_d or apparent K_d for a variety of proteins using the change in TNP-ATP fluorescence with binding.

Tables 1, 2, and 3 presents a list of proteins (mostly kinases) for which the dissociation constant (K_d) for both ATP and TNP-ATP has been published; additional examples from pre-2003 studies are presented in Hiratsuka's review (3). In the tables, the K_d for ATP binding ranges from micromolar to millimolar, whereas the K_d for TNP-ATP ranges from nanomolar to micromolar. With few exceptions, the affinity of proteins for TNP-ATP is 20–2000× higher than for ATP. This higher affinity of the fluorescent ATP analog can simplify the equations used to calculate an accurate K_d from competition binding assays (64,65). Some results suggest that TNP-ATP may actually bind separately or differently than ATP because of the inherent properties of the TNP moiety (e.g., CheA and Ca^{2+}-ATPase in the tables; see also ATP binding versus altered TNP-ATP binding to proteins). Some proteins possess two or more ATP binding sites, as is the case with CheA, cystic fibrosis transmembrane conductance regulator (CFTR), Ca^{2+}-ATPase, and F-type ATPases. For most experimental results presented in the tables, the interaction of TNP-ATP with the protein was measured as the increase in fluorescence intensity after binding; however, in some cases (reported in the column "Peak shift"), the expected blue shift was also reported. This blue shift varied from 0 to 15 nm. The increased intensity and blue shift should be reversed by adding ATP. Where a reversal of the blue shift was observed, it is reported in the tables as a negative number in brackets. The range of experimental parameters include temperature (4–30°C) and pH (range 6.5–8). Typically, the fluorophore was excited at 408 nm (range used, 400–520 nm), and changes in emission (λ_{em}) were monitored from 500 to 600 nm. As can be seen from the penultimate column in the first three tables, multiple techniques are often used to determine binding parameters. The next sections discuss table entries in sequence. Later sections present additional uses of TNP nucleotides, followed by problems and best practices for using TNP-ATP in binding experiments.

Enzymes and protein complexes

Table 1 summarizes experimental results in which the K_d of ATP and TNP-ATP were determined. These results are discussed below.

CheA and other protein kinases. A good example of using TNP-ATP to measure K_d is the work of Eaton and Stewart with the common bacterial protein CheA (27,28). CheA is a protein histidine kinase used by bacteria for chemotaxis and has binding sites that bind ATP or ADP as a stimulus for locomotion. In 1998, TNP-ATP and other ATP or ADP analogs were first used to measure binding affinity to CheA (66); it was found that CheA forms a homodimer that binds two ligands. Initial estimates suggested that both binding sites had similar binding affinities with a K_d ~1 μM. Several years later, Bilwes et al. (67), used TNP-ATP fluorescence with CheA and estimated $K_d < 0.01$ μM. This is surprisingly different from the earlier result, with the only obvious differences between the two studies being that the earlier group used CheA from *Escherichia coli* and included the reducing agent, DTT (dithiothreitol), whereas the latter group used CheA from *Thermotoga maritima* and excluded DTT.

The issue seems to have been resolved a decade later in a pair of studies by Eaton and Stewart (27,28) that reported the dimer binds two ligands with

TABLE 1 Summary of ATP binding data for some enzymes and protein complexes

Protein	Organism	K_d TNP-ATP (μM)	K_d ATP (μM)	K_d ratio ATP/TNP-ATP	Salts/buffers/detergents	pH/temperature	Peak shift ($\lambda_{ex}/\lambda_{em}$)	Techniques	Reference
CheA (protein histidine kinase)	recombinant (bacteria: *T. maritima*)	site 1: 0.0016, site 2: 22	site 1: 6, site 2: 5000	3750, 230	25 mM NaCl, 50 mM potassium glutamate, 25 mM Tris, 10% glycerol	7.5/4°C	NR (520/530–600)	F, SFF	(27,28)
PTK for EGFR	recombinant (human)	0.43 ± 0.22	47.0 ± 5.6	110	20 mM HEPES, 10% (v/v) glycerol	7.4/22°C	15 blue (418/500–650)	F, P32	(29)
MDD (GHMP kinase family)	recombinant (human); (yeast)	0.55 ± 0.02; 0.49 ± 0.04	Km = 690 ± 70; Kd = 169 ± 17	1250; 340	50 mM Tris, 1 mM DTT; 100 mM NaCl, 100 mM Tris	~7.4/30°C	6–15 blue (408/500–600)	F, XR	(30,31)
SPS	recombinant (bacteria)	1.22 ± 0.15	239 ± 3	200	100 mM NaCl, 30 mM KCl, 25 mM Tris	7.0/RT	10–15 blue (408/500–600)	F	(32,33)
PC	recombinant (bacteria: *R. etli*)	21 ± 3	5000 ± 400 (Hill = 3.1 ± 0.5)	240	100 mM Tris, 20 mM $NaHCO_3$	7.8/30°C	9 blue (408/500–600)	F, SFF	(34)
Hexokinase	yeast	2.6, 1.1 (+Glu)	1340, 230 (+Glu)	520; 210 (+Glu)	10 mM Tris	6.5–7.4/25°C	NR (405/520)	F, CD, IF	(35,36)
Nbp35-Cfd1 complex (cytosolic iron-sulfur cluster assembly scaffold)	yeast	0.190 ± 0.016	21 ± 6.4 (MANT-ATP); 43 ± 9 (BoATP)	110; 230	100 mM NaCl, 50 mM Tris, 10% glycerol	8.0/25°C	NR (469/555)	F, FA	(37)
TrwB (hexamer)	bacteria	1.2 ± 0.4	480	400	200 mM NaCl, 50 mM Tris, 0.1 mM EDTA, 20% glycerol, 0.05% (w/v) dodecyl maltoside	7.8/25°C	6 blue [−2] (410/560)	F	(38)

All entries include proteins for which the K_d (dissociation constants) was determined for both ATP and TNP-ATP. In some cases, K_d (ATP) was determined by competition against TNP-ATP, but in other cases it was determined independently. Methodologies used that are related to ATP-protein interactions are indicated in the penultimate column. Information on the protein is in the first two columns. K_d-values and ratios are in columns 3–5. Experimental conditions of the fluorescence experiments are in columns 6 and 7; however, chelators and divalent cations (e.g., Ca^{2+} and Mg^{2+}) are not listed because they varied greatly within individual experiments. Column 8 lists whether a shift in the TNP-ATP peak λ_{em} was observed or not reported after the addition of protein. Reported values are in nanometers, and "blue" indicates a shift to shorter wavelengths (hypochromic shift). In some experiments with a reported blue shift, sequential addition of ATP partly reversed the shift; in these cases, the extent of reversals (a red shift) is listed as a negative number in brackets. Numbers in parentheses are λ_{ex} and λ_{em} in nanometers; a range for λ_{em} indicates a spectrum was reported for the range indicated. The last two columns indicate techniques used in the work and the work's reference for measuring K_d. CD, circular dichroism; ChemL, chemiluminescence; F, TNP fluorescence; FA, fluorescence anisotropy; IF, intrinsic (tryptophan) fluorescence; MM, molecular modeling; NR, not reported or not relevant; P32, radiochemical assay with ^{32}P; RT, room temperature; SFF, stop-flow fluorescence; XR, x-ray crystallography.

TABLE 2 Summary of ATP binding data for some transport proteins and ion channels

Protein	Organism	K_d TNP-ATP (μM)	K_d ATP (μM)	K_d ratio ATP/TNP-ATP	Salts/buffers/detergents	pH/temperature	Peak shift ($\lambda_{ex}/\lambda_{em}$) (nm)	Techniques	Reference
Cdr1p (ABC transporter)	recombinant (yeast)	1.85 ± 0.13	76 ± 4	41	60 mM Tris	6.5/RT	4 blue (408/500–600)	F, IF	(39,40)
CpABC4 (ABC transporter)	recombinant (*C. parvum*)	7.04 ± 0.02	97.54 ± 22.4	14	50 mM Tris, 100 mM KCl, 0.02% HECAMEG (detergent)	6.8/25°C	NR (408/545)	F, IF	(41)
CFTR (domains NBD1 and NBD2)	recombinant (human)	NBD1: ~8, NBD2: ~11	NBD1: Ki = 6700 (competitively displaced), NDB2: Km = 300	NBD1: ~840, NBD2: ~27	50 mM Tris, 50 mM NaCl, 10% glycerol, 0.1 μM dodecyl maltoside	7.5/25°C	NR (410/550)	F, P32	(42,43)
CFTR-NBD2	recombinant (human)	7.17 ± 0.14	26.9 ± 1.6	3.8	50 mM Tris	7.5/25°C	NR (408/545)	F	(44); see also (45)
CFTR-NBD2 (P51)	synthetic 51 amino acids (human)	0.36	460	1280	20 mM HEPES	7.4/25°C	NR (400/540)	F, CD, ChemL	(46)
VNUT (organic anion transporter family)	recombinant (human)	4.8 ± 0.1	~6000	~1250	100 mM KCl, 20 mM MOPS, 20% glycerol, 0.02% DDTM (detergent)	7.5/15°C	5–6 blue [−2] (410/500–620)	F	(47)
TRPV1 (TRP channel family)	mammalian	1.01 ± 0.16	5300 ± 2100	5200	50 mM NaCl, 20 mM Tris	7.5/22°C	NR (462/527)	F, MM	(48)

See Table 1 legend for additional explanations and abbreviations.

TABLE 3 Summary of ATP binding data for some pumps and the three binding sites of the ATP synthase

Protein	Organism	K_d TNP-ATP (μM)	K_d ATP (μM)	K_d ratio ATP/TNP-ATP	Salts/buffers/ detergents	pH/temperature	Peak shift ($\lambda_{ex}/\lambda_{em}$) (nm)	Techniques	Reference
Ca^{2+}-ATPase from SR	rabbit (SR vesicles)	CS: 1.0, RS: 0.6	CS: 2.4, RS: 2500	CS: 2.4; RS: 4200	100 mM KCl, 20 mM Tris, 20% glycerol, CPK + CP	8.0/25°C	12 blue (418/538)	F, SFF, P32	(6,49), see also (50)
Ca^{2+}-ATPase (p48, SERCA1)	recombinant (cytoplasmic domain, rabbit SR)	7.7 ± 1.7	Ki = 1400 (competitively displaced)	180	100 mM KCl, 20 mM MOPS, 3 mM DTT	7.25/RT	NR (410/540)	F, CD	(51)
H,K-ATPase	hog stomach	<0.025	86	>3400	40 mM Tris	7.4/RT	10 blue (405/500–625)	F, P32	(52,53)
Na,K-ATPase (part)	recombinant	3.1 ± 0.2	6200 ± 700	2000	50 mM Tris	7.5/22°C	NR (462/527)	F, MM	(54,55) see also (56)
H-ATPase	recombinant (yeast)	6.5	3000	460	50 mM MOPS	7.0/RT	NR (408/550)	F, P32	(57)
F-ATPase	beef heart mitochondria	Ki for hydrolysis: ATP: 0.005, ADP: 0.01; synthesis Ki (both): 1.3	NR	NR	250 mM sucrose, 40 mM MES, 40 mM Tris, 1 mM KH_2PO_4	7.5/RT	NR (436/>460 with cutoff filter)	F, P32	(5,58)
F1 ATPase (α- and β-subunits)	recombinant (*Bacillus sp.* PS3)	7.5 (0.002 for TNP-ADP)	NR	NR	20 mM tricine	8.0/NR	NR	difference spectra	(59)
F1 ATPase	mitochondria	0.2 (third binding site)	2000 (third binding site)	10,000	250 mM sucrose, 50 mM Tris, 20 mM Pi	8.0/RT	NR	P32	(60) see also (10)
F1 ATPase	*E. coli*	<0.003, 0.26, 1.9	0.02, 1.4, 28	>6.7, 5.4, 15	50 mM Tris	8.0/23°C	NR	quench of IF by TNP, FA	(61,62)
V-ATPase	yeast (*Saccharomyces cerevisiae*)	0.16 ± 0.05	NR	NR	150 mM NaCl, 25 mM Tris, 0.5 mM DTT	7.9/10°C	NR (465/485–600)	F, XR	(63)

See Table 1 legend for additional explanations and abbreviations. CS, catalytic site; RS, regulatory site.

markedly different affinities. The high-affinity site has a K_d of 0.0016 μM, and the low-affinity site has a K_d ~10,000× weaker (Table 1). However, it remains unclear why a homodimer like CheA would exhibit different binding mechanisms for the same molecule (27).

Another kinase studied with TNP-ATP is the protein tyrosine kinase (PTK) intrinsic to the epidermal growth factor receptor (EGFR). This kinase phosphorylates itself on a tyrosine residue after activation. It was found that TNP-ATP bound ~100× tighter than ATP and was a "functional substrate," but the V_{max} for hydrolysis was 200 times slower than with ATP (29).

Mevalonate diphosphate decarboxylase (MDD) is a member of the GHMP kinase family, whose members include galactokinase, homoserine kinase, mevalonate kinase, and phosphomevalonate kinase. Binding of TNP-ATP to human MDD caused an ~3-fold increase in intensity and a blue shift of 6–7 nm (30), whereas the yeast MDD caused a >6-fold increase in intensity and a blue shift of 15 nm (31). This later group looked at how point mutations at a critical site altered binding of TNP-ATP.

Synthetase, carboxylase, and hexokinase. Another bacterial-derived ATPase studied with TNP-ATP is the selenophosphate synthetase (SPS). Like CheA, SPS has two binding sites for TNP-ATP, although only one appears to be catalytically active for ATP (32), with a reported K_d as listed in Table 1 (33). The other TNP-ATP binding site appears to have an affinity at least 10 times lower (32). The high-affinity site has a K_d between the K_d of the two CheA sites, and the affinity of SPS for TNP-ATP is more than 100× higher than for ATP, as it is for both CheA sites.

Pyruvate carboxylase (PC) is an enzyme that hydrolyzes ATP in the liver gluconeogenesis pathway. Using PC from the bacteria *Rhizobium etli*, Adina-Zada and co-authors (34) found that TNP-ATP binds to, but is not hydrolyzed by, PC. Similar to other proteins listed in Table 1, TNP-ATP binds to PC with >1000× higher affinity than ATP; however, their data suggest that TNP-ATP binds at a location separate from the ATP binding site. They show that TNP-ATP appears to be an allosteric activator of PC, which implies that TNP-ATP can and does bind to sites on proteins that are not ATP binding sites.

One yeast ATPase studied with TNP-ATP is hexokinase, the enzyme that phosphorylates sugars such as glucose. With this kinase, it was observed glucose binding increases affinity for ATP by ~2.5× and its affinity for TNP-ATP by ~6× (35,36). Several points are noteworthy in the Arora et al. study (36): 1) TNP-ATP could be hydrolyzed by hexokinase producing TNP-ADP, although at a much slower rate than ATP hydrolysis; 2) the ADP and AMP analogs were also tested, and the following order of interactions was found: TNP-ATP > TNP-ADP >>> TNP-AMP; and 3) fluorescence enhancement after binding of TNP-ATP to hexokinase was reduced if ATP was added first. These results, combined with data from a 50-amino acid peptide from hexokinase, support the conclusion that TNP-ATP binds at the ATP binding site. It also shows that valuable information can be obtained by comparing different TNP nucleotides, which will be discussed later.

Protein complexes. Nbp35 and Cfd1 are yeast proteins that can combine to form a scaffold for cytosolic iron-sulfur cluster assembly. This scaffold hydrolyzes ATP in processing iron-sulfur clusters. Grossman et al. (37) used TNP fluorescence to determine the K_d of the Nbp35-Cfd1 complex for TNP-ATP and then used fluorescence anisotropy to determine the K_d for two other fluorescently labeled ATPs: MANT-ATP (N-methylanthraniloyl-ATP) and BoATP (BODIPY-FL 2′/3′-O-[N-(2-aminoethyl)urethane] ATP). They report a K_d for TNP-ATP that is more than 100× tighter than the K_d for either MANT-ATP or BoATP (Table 1).

TrwB is one of a group of membrane proteins involved in bacterial conjugation (68). Both TrwB (38) (Table 1) and TrwD (69) (referenced in Table 4) are ATPases that have been studied with TNP-ATP. Both proteins have a much higher affinity for TNP-ATP over ATP, and in both cases, a significant blue shift was observed with binding TNP-ATP.

Transport proteins and ion channels

Table 2 summarizes experimental results in which the K_d of ATP and TNP-ATP were determined for transport proteins and ion channels. These results are discussed below.

The yeast *Candida* drug resistance 1 protein (Cdr1p) and the parasitic protozoan protein *Cryptosporidium parvum* ABC transporter 4 (CpABC4) are both members of the ATP binding cassette (ABC) transporter family of proteins. Both proteins have a fairly low affinity for ATP (K_d of 75–100 μM) (39,41), consistent with the intracellular concentration of ATP. CpABC4 binds TNP-ATP with only ~14× higher affinity than ATP and has been shown to hydrolyze TNP-ATP (41), whereas Cdr1p binds TNP-ATP with ~40× higher affinity (39,40).

The CFTR is a chloride channel that is also a member of the ABC transporter family. It has two nucleotide binding domains, NBD1 and NBD2. As shown in Table 2, ATP and TNP-ATP binding to these domains has been measured for the whole protein as well as the individual domains (42–46). Similar to other proteins discussed above, NBD1 binds ATP in the millimolar range and binds TNP-ATP 1000× tighter. NBD2 has a similar

TABLE 4 Examples of proteins reported to interact with TNP nucleotides

Protein	Organism	TNP nucleotides used	Observations (concentrations in μM)	Salts/buffers/ detergents	pH/temperature	Peak shift ($\lambda_{ex}/\lambda_{em}$) (nm)	Techniques	Reference
GluT1 (glucose transporter)	human	ATP	modulates sugar transport	PBS	6.0–7.4/20°C	NR (408/540)	SFF	(70)
PriA (helicase)	bacteria (*E. coli*)	ATP, ADP	Kd site 1: 0.67 ± 0.22; site 2: 53 ± 17	20 mM NaCl	7.0/20°C	NR (408/550)	SFF, F; IF, F	(71,72)
RepA (helicase)	bacteria (*E. coli*)	ATP, ADP	Kd ~2.1 ± 0.4 (10°C); 2.0 ± 0.4 (20°C)	10 mM NaCl, 50 mM Tris, 10% glycerol	7.6/10°C, 20°C	NR (410/560)	SFF	(73)
ABCF3 (ABC superfamily)	mammalian	ATP, ADP, AMP	K1/2 2.6 ± 0.1, Hill = 1.8 (displaced with 0.1 mM ATP)	PBS, 20% glycerol	7.4/RT	6 blue (403/ 450–600)	F	(74)
CDKA (cyclin-dependent kinase)	recombinant (plant: maize)	ATP	Nitration lowers ATP binding	PBS, 160 mM imidazole	NR/25°C	11 blue [~−11] (495/540)	F, MS	(75)
Porin 31 (voltage-dependent anion-selective channel)	human and bovine	ATP	NR	50 mM Tris-HCl	7.4	5 blue (410, 450–575)	F, P32, AC	(76)
CpABC3 (ABC transporter)	recombinant (*Cryptosporidium parvum*)	ATP	Ki 36.6 ± 4.5 (inhibition of ATP hydrolysis by TNP-ATP)	100 mM KCl, 50 mM Tris, 0.02% HECAMEG (detergent)	6.8/20°C (F); 7.5/37°C (HPLC)	0 blue (408/ 520–600)	F, IF	(77)
VC1:IIC2 and ACI (adenylyl and guanylyl cyclases)	recombinant (human)	ATP, ADP, AMP, GTP, GDP, UTP, CTP	Ki (VC1:IIC2) 3.3 ± 1.4; (ACI) 0.009 ± 0.004	100 mM KCl, 25 mM HEPES	7.4/25°C	14 blue (405/500–600)	F, P32, MM	(78)
SaUspA (stress protein)	Archaea (*S. acidocaldarius*)	ATP	Kd 7 ± 2, Hill = 0.84., Kd (G97A) = 350	150 mM NaCl, 50 mM Tris	8/25°C	NR (409/540)	F	(79)
Kir6.2 (KATP channel)	human	ATP, ADP	washout of TNP-ATP nucleotides; inhibition by epoxyeicosatrienoic acids	140 mM KCl, 10 mM HEPES	7.4/RT; 7.5/23°C	NR (FRET/565, 403/546)	F, FRET, ePh	(80) see also (26,81)
TrwD (secretion ATPase superfamily)	bacteria	ATP	Kd, apparent Km 11	200 mM NaCl, 20 mM HEPES, 5% glycerol	7.6/21°C	13 blue (407/ 475–625)	F, CD, MM; P32	(69,82)
FBPase	human liver	AMP	Kd 13.1, IC50 = 7.4 ± 0.7	50 mM Tris	7.4/37	10 blue [−3] (410/500–630)	F, CD, MM	(83,84)
PilB-ATP (506–890) (type IV assembly ATPase)	recombinant (*T. thermophilus*)	ATP, ADP	Kd 42 (80 for TNP-ADP)	135 mM NaCl, 25 mM Tris, 2.5% glycerol, 2 mM TCEP	7.4/NR	NR (405–550)	F, XR	(85)

Includes the nucleotide(s) and buffer conditions used and the reported interaction measured. ePh, electrophysiology. See Table 1 legend for additional explanations and abbreviations.

affinity for TNP-ATP but binds ATP more tightly than NBD1.

The vesicular nucleotide transporter (VNUT) is a member of the organic anion transporter family. VNUT uses a membrane potential to transport nucleotides such as ATP across membranes. In carefully performed fluorescence experiments, Iwai et al. (47) showed that TNP-ATP competitively binds to the ATP binding site (K_d ~5 μM) with a 1000× higher affinity than ATP (K_d ~6 mM).

TRPV1 (transient receptor potential channel V1) is a nonselective cation ion channel that responds to hotter temperature and acidic conditions to produce a pain response. TRPV1 is one of the most extreme examples of TNP-ATP binding tighter than ATP. The ratio $K_{d(ATP)}$ to $K_{d(TNP\text{-}ATP)}$ is greater than 5000× (Table 2).

Pumps and the ATP synthase

Table 3 summarizes experimental results in which the K_d of ATP and TNP-ATP were determined for pumps and the ATP synthase. These results are discussed below.

Ca^{2+}-ATPase. TNP-ATP has been used extensively to better understand the nature of the affinity for ATP of the sarco/endoplasmic reticulum calcium-ATPase (SERCA). This Ca^{2+}-ATPase hydrolyzes ATP to transfer calcium ions from the cytosol of muscle cells back into the sarcoplasmic reticulum (SR). It belongs to the P-type ATPase family of membrane proteins. Early experiments studied the Ca^{2+}-ATPase in vesicles isolated from muscle SR (6,7,49,86–88). These experiments reported strong ATP binding at a catalytic site ($K_d = 2.4$ μM) and lower affinity to a separate regulatory site ($K_d = 2500$ μM, Table 3). TNP-ATP had a high affinity to both sites ($K_d = \sim 1$ μM) and was hydrolyzable. Binding at the catalytic site is an early example of the rarely reported case in which TNP-ATP and ATP have similar binding affinities. Further studies with the monophosphate nucleotide, TNP-AMP, bound to the Ca^{2+}-ATPase showed changing fluorescent intensities that correlated to the state of ATP hydrolysis that the enzyme was in (7,89–93). Thus, TNP-AMP fluorescence became a marker for this protein's conformation. The conformation(s) that made the TNP-AMP binding pocket most hydrophobic gave the greatest fluorescent intensity, and this enhanced fluorescence was referred to in these publications as “superfluorescence” (this is not the usual use of the term superfluorescence, which is a quantum optics phenomenon in which a group of molecules becomes excited together and emits a brief bright pulse of light).

Later experiments studied the binding of ATP and TNP-ATP to “p48,” a recombinant protein containing just the cytoplasmic domain of the Ca^{2+}-ATPase (expressed in *E. coli*) (51,94). Those results were consistent with the regulatory site having more than 1000× higher affinity for TNP-ATP than for ATP (Table 3).

Other P-type ATPases. In addition to the Ca^{2+}-ATPase, the family of P-type ATPases includes most ion pumps, such as the H,K-ATPase, Na,K-ATPase, and H-ATPase. The H,K-ATPase is the pump responsible for acidifying the stomach. Similar to the initial studies on the Ca^{2+}-ATPase, Faller used TNP-ATP with vesicles containing the acid pump isolated from the stomach of hogs (52,53). Those studies (Table 3) identified unusually strong binding of ATP to the H,K-ATPase ($K_d = 0.086$ mM), and still TNP-ATP bound over 3000× tighter ($K_d < 25$ nM).

The Na,K-ATPase is one of the most ubiquitous pumps and is responsible for maintaining the Na^+ and K^+ gradients across neuron, muscle, and many other cell types. Amler's group (54) used the recombinant protein coding for the ATP binding site (H4-H5 loop) of the Na,K-ATPase and found that the K_d for ATP and TNP-ATP were 6.2 mM and 3.1 μM, respectively, with TNP-ATP binding 2000× tighter (Table 3). Their results took advantage of an improved and simplified set of equations used to calculate K_d (64,65). Earlier experiments by Pratap et al. (95) measured five rate constants associated with TNP-ATP binding to the Na,K-ATPase, and Moczydlowski (96) observed that TNP-ATP was not hydrolyzed by the ATPase.

Another member of the P-type ATPase family is the proton-pumping H-ATPase. Expressing just the major hydrophilic domains from a yeast H-ATPase, Capieaux et al. (57) determined the binding of ATP and TNP-ATP to these domains. Consistent with the similarity between the H-ATPase and the Na,K-ATPase (97), the reported K_d-values are also similar (Table 3), with binding of TNP-ATP over 400× tighter compared to ATP.

ATP synthase, including F- and V-type ATPase. Almost all of the proteins listed in the previous tables show a much higher (>100×) affinity for the ligand TNP-ATP compared to ATP. This suggests that the TNP moiety strongly contributes to the binding of the ligand with the protein. However, the catalytic site of the Ca^{2+}-ATPase and the F-ATPase are exceptions to this pattern (Table 3). In both proteins, TNP-ATP binds with only slightly higher (<10×) affinity compared to ATP (59,61,62,98,99). The F-ATPase is a mitochondrial and bacterial membrane protein formed of many subunits that together act as a molecular motor. It generally functions as a synthase but can run in reverse as a hydrolase (H-ATPase). When operating as a synthase, it uses the pH gradient across the membrane to induce rotation of its γ-subunit with respect to a ring of three pairs of α- and β-subunits. This movement catalyzes the formation of ATP from ADP and P_i. There

are three ATP/ADP binding pockets between each set of α- and β-subunits. This adds to the complexity of measuring ligand affinity (similar complications are seen in dimer formation with CheA discussed above). Binding experiments were performed with just the α-subunit, just the β-subunit, and both (59,98,100–102). When TNP-ATP is added to the functional F-type ATPase protein complex (including both α- and β-subunits), it greatly slows both the synthesis and hydrolysis activity with an extremely low K_i of 5–10 nM, Table 3 (5) see also review by Hong and Pedersen (103). The K_d for sequential binding of three ATP to the mitochondrial F1-ATPase were first reported as 1.6, 0.4, and 55 μM (104), although the interpretation leading to these values was debated, with a K_d for binding of the first ATP reported as 1 pM or 10^6 times tighter (105,106). It should be noted that a K_d in the picomolar range is difficult to measure, especially under conditions in which the protein was almost certainly at a higher concentration. The latter group also reported the K_d for ADP binding as 0.28 μM. More recently, Weber's group has reported binding for the three binding sites in *E. coli* as 0.02, 1.4, and 28 μM, and in all cases the binding of TNP-ATP was only ~10$\times$ tighter. A similar binding story is likely true for the V-type ATPase, which is reported to bind TNP-ATP with a K_d of 0.16 μM (63). For many proteins, their strong affinity for TNP-ATP over ATP is likely due to direct interactions of the TNP moiety with the protein. In the case of the ATP synthase, for which a smaller increase is seen, we speculate that this is due to a very tight fit for the ATP, ADP, and P_i ligands necessary for efficient catalysis of the synthase reaction, leaving little room for the TNP moiety.

The data in Tables 1, 2, and 3 discussed above show that TNP analogs continue to contribute to the understanding of many ATP binding proteins and make clear that TNP-ATP does not bind to proteins with the same affinity as ATP. Therefore, TNP-ATP cannot be used as an ATP analog for estimating the K_d of ATP directly. However, the K_d for ATP can be estimated through competitive inhibition of TNP-ATP binding using ATP. In the next section, additional applications for TNP-ATP are discussed.

Other uses for TNP nucleotides

In addition to using TNP-ATP as part of determining the K_d for ligand binding, TNP-ATP has been used to study other aspects of binding, including kinetics (on and off rates), inhibitory block (K_i and IC50) (107), and the Michaelis constant (K_m), for example. Another common use of TNP-ATP is as an antagonist of P2X receptors, as reviewed in (108) (see also (17,18,109,110)), and it continues to inspire the design of new P2X receptor antagonists (111). TNP-ATP is also useful in screening proteins for ATP binding (97,112–115). Several studies have compared the binding properties of TNP-ATP with other TNP-linked nucleotides such as TNP-ADP, TNP-AMP, and TNP-GTP. For example, in 1986, Biswas et al. (116) measured binding (K_m) to a DNA binding protein in *E. coli* and observed that TNP-ATP and TNP-ADP bound much more tightly than TNP-AMP. Additional examples are presented in Table 4.

Additional examples of proteins reported to interact with TNP nucleotides

Table 4 summarizes data from experiments in which TNP was attached to other nucleotides and used to measure other binding interactions such as regulation or inhibition.

Some proteins are regulated by ATP and TNP-ATP has been used to study this process. For example, Cloherty et al. (70) found "that TNP-ATP substitutes for ATP in nucleotide modulation of sugar transport" by the GluT1 sugar transporter in human red blood cells. They used an assay that combines the use of TNP-ATP and ATP to test whether or not the binding of ATP to the transporter is cooperative, using stop-flow fluorescence to test the timing of TNP-ATP binding to their protein. Stop-flow fluorescence has similarly been used by others (28,34,71,73,117,118).

An example of using multiple TNP nucleotide analogs to study protein binding properties is with the Ca^{2+}-ATPase, the pump that moves calcium from muscle cytoplasm into the lumen of the SR. In humans, there are three major variants of this pump, known as SERCA1–SERCA3. This pump hydrolyzes ATP (but not TNP-ATP) and binds ATP, ADP, and AMP with differing affinities. TNP analogs of all three nucleotides (i.e., TNP-ATP, TNP-ADP, and TNP-AMP) have been used to bind SERCAs and lock them into different conformations associated with their hydrolysis and pumping cycles (for reviews, see (119,120); see also (121–124)).

Another impressive finding among recent reports of using TNP-ATP in protein binding studies is the work of Peterson et al. (74). In their study of TNP-ATP binding to ABCF3 (a member of the ABC superfamily of membrane transporters; Table 4), they observed the expected increase in fluorescence intensity and blue shift. But in contrast to many other proteins for which $>$2 mM ATP was needed to partly compete off TNP-ATP, including many shown in Tables 1, 2, and 3 (see also (125)), these authors observed a significant decrease in fluorescence after the addition of just 0.1 mM ATP (although it was not reported if the blue shift reversed). The same concentrations of ADP and AMP were less potent in competing with TNP-ATP.

ABCF3 actually has two NBDs that are reported to be cooperative, such that ATP binding to one domain increases the affinity of the other NBD (74).

A recent novel use of TNP-ATP was to show that ATP binding was lowered after nitration of two tyrosines in the binding pocket of the CDKA;1 protein (75). CDKA is a member of the cyclin-dependent kinase A family that helps regulate the cell cycle in plant cells. It is noteworthy that when using the recombinant protein, the addition of 1 mM ATP caused nearly complete reversal of the blue shift and intensity increase that were originally observed after addition of 10 μM TNP-ATP. This suggests that TNP-ATP binding was not as tight as observed with many other proteins.

Other methods to confirm TNP-ATP binding data

An important point illustrated and acknowledged by the early Hiratsuka and Uchida (4) study is that the kinetics of TNP-ATP binding to a protein are different than the kinetics of ATP itself binding to a protein. Thus, it is important to find ways to determine the binding parameters of ATP without relying exclusively on the data from TNP-ATP binding. For example, in studying porin 31, a voltage-dependent anion-selective channel, Florke (76) observed that TNP-ATP fluorescence increased in intensity and blue shifted, consistent with binding to porin (Table 4). This they confirmed by three additional methods: 1) affinity chromatography using ATP-agarose, 2) using the radiolabel ^{32}P-ATP, and 3) showing that TNP-ATP binds to a peptide from the protein. A second example is the work of Fischer et al. (126) on the P2X receptor channel. Here, it was known that TNP-ATP is an inhibitor of P2XR, and its binding was used to characterize the effect of point mutations on binding. Results were confirmed by structural bioinformatics-driven modeling. A third example is from Kadenbach's group working on multiple ATP binding sites in cytochrome c oxidase, for which [^{35}S]ATPαS was used to confirm K_d data obtained with TNP-ATP (127,128). Some of the different methods used in combination with TNP-ATP are listed under the "Techniques" column in all the tables.

Additional fluorescent tags. An additional way to confirm binding data obtained with TNP-ATP is to use a different tag (for example, see Protein complexes). Although all will have the same kind of problems, e.g., an extra group that will enhance or interfere with ATP binding, each will do so differently and provide a broader view of the interaction of ATP with proteins. Many fluorescent tags have been made and attached to either ATP (e.g., εATP or etheno-ATP) or other nucleotides; one more commonly used tag is MANT (N-methylanthraniloyl) (8,24,37,78,129–133). Whereas εATP is modified on the adenosine ring of ATP, MANT and TNP are attached to the ribose sugar. MANT is distinctive in that it is attached with one, not two, bonds so it can rotate freely and perhaps allow ATP to bind more naturally (130,131). On the other hand, MANT as a fluorescence molecule is less desirable because it must be excited in the ultraviolet and has a smaller signal/noise ratio than TNP (78).

Intrinsic tryptophan fluorescence. Another method to confirm TNP-ATP binding data is to use tryptophan fluorescence. Tryptophan is an amino acid found in most proteins that is fluorescent. Changes in tryptophan fluorescence can indicate changes in how a protein folds and interacts with its environment; however, its use is limited because its fluorescence is weak and quickly bleached. Lawton et al. (77) used tryptophan fluorescence in their attempts to characterize the ATP binding domain of CpABC3, a protein associated with multidrug resistance in an intestinal parasite. As in other studies with TNP-ATP, they found that the fluorescence intensity of TNP-ATP increased upon addition to their protein (indicating binding), but they were unable to compete off the TNP-ATP with ATP. However, they were able to confirm binding of ATP as a change in tryptophan fluorescence. Additionally, they showed that TNP-ATP acted as a competitive inhibitor of ATP hydrolysis by H6-NBD1, a recombinant fragment from CpABC3 (Table 4). Additional examples using intrinsic fluorescence are listed in each table (see IF under the "Techniques" heading). Another aspect of measuring intrinsic tryptophan fluorescence is when there is no change in fluorescence after ATP addition. This result suggests at least two possibilities: either ATP is not interacting with the protein or the conformational change that occurs when ATP binds to the protein is not causing a sufficient change in the environment of tryptophan to have a detectable change in its fluorescent properties. Clearly, it is informative to use a second method in addition to TNP-ATP fluorescence to verify the binding of a protein of interest to ATP.

Summary of past results and techniques

The uses of TNP-ATP are many and diverse, but most of them take advantage of the fluorescence properties of TNP-ATP that were noticed but only mentioned in the first reported use by Hiratsuka and Uchida (4). Many researchers use TNP-ATP to ascertain how ATP interacts with proteins, and several detailed protocols have been published (8,9). In many cases, other methods are also used.

TNP-ATP fluorescence is also used to discover information about the conformation of binding sites (e.g., the "superfluorescence" reported when TNP-AMP binds to Ca^{2+}-ATPase), which provides a valuable

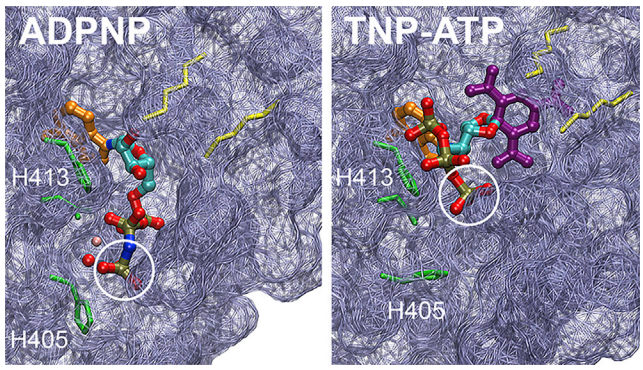

FIGURE 2 Abnormal binding of TNP-ATP to CheA. The crystal structure of CheA (*gray* mesh) binding with ADPNP (*left*) and TNP-ATP (*right*) is shown. Orange color highlights the adenosine ring deep within the binding pocket of both structures. The white circles mark the terminal phosphate for reference. Residues important for ATP binding and hydrolysis are highlighted in green. On the left, ADPNP is used to represent ATP. The pink sphere represents Mg^{2+}, which is coordinating the binding of water (*red sphere*), the terminal phosphate, and His405. On the right, TNP-ATP is within the binding pocket; purple highlights the TNP moiety. The yellow residues are lysine amino acids that move away from the binding pocket and interact with the TNP ring. Unless otherwise noted above, red represents oxygen, blue represents nitrogen, tan represents phosphorus, and cyan represents carbon atoms. Crystal structure from (67). Images created using Visual Molecular Dynamics (136), version 1.9.4a51, with coordinates from the Protein Data Bank: PDB: 1i59 (ADPNP) and PDB: 1i5D (TNP-ATP).

method for understanding the hydrophobicity of the binding pocket of a protein. However, the differences in binding properties for TNP-ATP versus ATP usually necessitate the use of a second method to determine binding characteristics, such as the use of tryptophan fluorescence, ^{32}P-labeled ATP, or x-ray crystallography, to better understand how ATP interacts with a protein of interest.

Problems with TNP-ATP

From the above discussion, it is clear that TNP-ATP can provide important information on the properties of ATP binding proteins. However, care must be exercised to correctly interpret the changes in fluorescence spectra obtained from TNP-ATP interacting with a particular protein. The next sections highlight some problems relevant to any studies in which the TNP moiety has been attached to a nucleotide such as ATP. The most apparent consideration to take into account when using TNP-ATP is that it typically binds much more tightly to proteins than ATP itself does. It was formulated to be similar to ATP, but it is not the same molecule because of the fluorophore attached to the ribose sugar of ATP (Fig. 1). These considerations, when not accounted for, may lead to misinterpretation of the data. However, the high affinity of TNP-ATP allows the use of simplified equations to calculate K_d from competition experiments (64,65).

ATP binding versus altered TNP-ATP binding to proteins

Another consideration in using TNP-ATP is how it interacts with proteins compared to ATP. Bilwes et al. (67) asked this question with respect to CheA and found that CheA cannot hydrolyze TNP-ATP, thus making TNP-ATP a competitive inhibitor for ATP binding to CheA. Likewise, it has been shown that the P2X receptor is antagonized by TNP-ATP (134). With both proteins, it was confirmed using crystallography (67,135) that TNP-ATP binds differently compared to ATP (see Fig. 2). Bilwes et al. concluded that TNP-ATP's unique sugar residue conformation directs the phosphates away from the ATP/ADP binding site, and consequently, only one hydrogen bond forms (rather than the expected three) between TNP-ATP and His 413 of CheA. The TNP ring binds to a hydrophobic pocket near the CheA ATP binding site that causes this shift away from the ATP binding site and prevents hydrolysis (Fig. 2). Kasuya et al. (135) proposed that with the P2X7 receptor channel, the TNP moiety also interacts with the protein to prevent complete opening of the channel. Consequently, TNP-ATP is a competitive inhibitor that binds with different chemistry from ATP. Bilwes et al. concluded that despite the noted differences between ATP/ADP and TNP nucleotide analogs, there were still uses for TNP-ATP in CheA analysis.

In contrast and as noted earlier, TNP-ATP has been shown to be a substrate for several other enzymes, including F_1-ATPase (58) and CpABC4 (41). TNP-ATP was also hydrolyzed, but at a greatly reduced rate, by hexokinase (36), PTK for EGFR (29), and P-glycoprotein multidrug transporter (137).

Unexpected spectral changes

The typically higher affinity of TNP-ATP for ATP binding proteins (and others) can make it difficult to confirm it is binding at an ATP binding site. This is why a chief consideration in whether or not an experiment has successfully shown TNP-ATP binding to an ATP binding site is whether or not ATP was able to compete the TNP-ATP out of the binding site. When TNP-ATP binds to a protein, its fluorescence increases and its peak wavelength shortens (blue shift). Successful competition is shown when excess ATP restores TNP-ATP fluorescence to its original (lower) intensity and longer wavelength (red shift). In practice, it is easier to measure changes in intensity than in the peak wavelength, so intensity changes are often the only reported parameter. Additionally, because TNP-ATP binding is usually much tighter, high concentrations of ATP may be required to compete TNP-ATP off. Hence, a complete

reversal of the fluorescence spectra is seldom observed, confounding interpretation of binding experiments. A lack of reversal can also indicate nonspecific binding of TNP-ATP such that there is no competition from ATP. In a study of the Na^+/K^+-ATPase, Pratap and co-workers observed both specific and nonspecific binding of TNP-ATP (95,118).

For these and other reasons, it is often desirable to measure changes in the peak wavelength, λ_{em}, which, in contrast to intensity changes, has fewer confounding factors that cause artifactual shifts. However, even if the peak wavelength change does reverse after the addition of ATP (or another molecule), it is possible that ATP is releasing TNP-ATP through an allosteric conformational change, as seen with PDK1 (9).

Spectral shifts and intensity changes become even harder to interpret properly if the fluorescence intensity of TNP nucleotides is measured at only a single wavelength. In this case, a shift in λ_{em} will mistakenly be observed as a change in intensity at the measured wavelength. A simple way to avoid this problem is to take the integrated intensity over a wide emission spectrum, as done by Eaton and Stewart (27,28). Although this prevents a shift in λ_{em} causing a change in measured intensity, it loses the useful information of observing the expected blue shift after TNP-ATP binding and restorative red shift when competed off by ATP.

Additionally, many confounding factors unrelated to TNP-ATP binding can cause a decrease in intensity, including dilution, bleaching, inner-filter effects, quenching, formation of precipitates, structural changes within the protein, and environmental changes (e.g., pH and ionic composition). With normal care, dilution effects can be minimized or corrected for, and bleaching is generally not a problem with TNP fluorescence. The inner-filter effect occurs when higher concentrations of absorbing compounds are used during fluorescence measurements (138). When these compounds (e.g., TNP-ATP $>$ 10 μM, protein or ATP) attenuate the excitation beam, there is a reduced emission. (Light absorption by high concentrations of absorbing compounds is known as the primary inner-filter effect; the secondary inner-filter effect happens when excitation and emission spectra overlap, which is not usually a problem with TNP-ATP.) Large protein aggregates or precipitants can cause similar problems by absorbing or scattering the light beam and thus reducing the measured emission spectra. Quenching is generally not a problem if [TNP-ATP] $<$ 40 μM (70), and TNP-ATP is typically used in the 1–10 μM range, although 100 μM has been used with apparent success in 96-well microplates containing a total volume of just 200 μL (139). Changes in TNP-ATP fluorescent intensity can also occur if there is a change in the hydrophobicity of the ligand binding pocket within the protein. This latter intensity change was used diagnostically with the Ca^{2+}-ATPase to distinguish protein conformational states associated with the enzymatic reaction cycle (see Ca^{2+}-ATPase).

Two examples help demonstrate some of these complications. In both cases ATP was added to a solution containing TNP-ATP bound to protein. In the first, fluorescent intensity unexpectedly increased after the addition of ATP, and in the second, the intensity decreased, but the peak wavelength was blue shifted instead of the expected red shift. In both examples, something unusual must be happening.

Example 1: unexpected increase in fluorescence. When the ATPase from SR (Ca^{2+}-ATPase), isolated in vesicles, was added to 5 μM TNP-ATP, strong binding was observed as an increase in fluorescence intensity (86). But when 10-fold excess ATP was added to displace TNP-ATP, fluorescence unexpectedly increased 3$\times$ with an apparent blue shift. Assuming that TNP-ATP was already bound to the ATPase, addition of ATP should have displaced TNP-ATP from the hydrophobic binding pocket back into the solution, thereby lowering the fluorescence intensity. Indeed, the authors showed that some of the TNP-ATP had been displaced by the excess ATP using radiolabeled TNP-[γ^{32}]ATP. From these data, the authors conclude that after adding ATP, "the observed fluorescence enhancement must be due to a conformational change in the environment of the binding site consequent to phosphorylation by ATP" (86). This illuminates a potential and subtle complication of using TNP-ATP as a fluorescent ATP analog. It is possible to get an unexpected finding in which TNP-ATP fluorescence is enhanced upon the addition of ATP instead of decreased even though some TNP-ATP has been displaced.

This finding of increased fluorescence with ATP addition was also confirmed in a later work in which TNP-ATP fluorescence was used to understand enzyme kinetics of the Ca^{2+}-ATPase (49). Additionally, they found that adding inorganic phosphate also increased TNP-ATP fluorescence, suggesting that phosphorylation was not required for the increased fluorescence. Adding inorganic phosphate caused a 12 nm blue shift. However, they did find that adding 50 mM KCl caused a decrease in TNP-ATP fluorescence, and this finding was later confirmed and elaborated upon (140). These researchers also examined other monovalent cations (Rb^+, Cs^+, Na^+, and Li^+) and found that potassium created the most pronounced decrease in fluorescence. This suggests that changes in salt concentrations change the spectra. Although these results may be limited to just the Ca^{2+}-ATPase, it has been shown that pH alters TNP-ATP fluorescence intensity (12) and peak

wavelength (see Fig. 3). Measurements by Ye et al. (11) of TNP-ATP spectral properties showed that in 87% glycerol, TNP-ATP fluorescence intensity and apparent molar extinction coefficient increased with pH, but fluorescence lifetimes did not. Consistent with previous data (141,142), this apparent change in molar extinction coefficient "was attributed to the pH-induced change in equilibrium between two species of TNP-ATP," each with different extinction coefficients (11). In the normal course of fluorescence experiments, unanticipated pH changes can happen when solutions of concentrated ATP (often acidic) are added to the reaction cuvette. In most reports, it is not clear whether pH was checked after the last sequential addition of ATP. It is reassuring when it is reported, as done by Kubala and colleagues, that the "buffer pH was adjusted to 7.5 after addition of ATP" (48,54).

Example 2: unexpected fluorescence blue shift. Sometimes adding ATP to a solution containing protein-bound TNP-ATP does lower the fluorescence intensity, as expected, but an inspection of the spectra shows a blue shift instead of the expected red shift. An example of this comes from a 2008 study by Chavali et al. (143). This study attempts to characterize a segment of the RNA genome of a virus by translating it into a protein called P68 and performing several assays on the protein. The authors claim that P68 has ATP binding activity because they are able to see a fluorescent intensity increase after adding protein at a concentration of 1 μM to a 5 μM solution of TNP-ATP. They did not report whether there was a shift in the fluorescent peak of TNP-ATP after adding the protein, but a careful inspection of their data (redrawn in Fig. 4) suggests a 2 nm blue shift, small but likely significant. They then show that adding 15 mM ATP (a 3000-fold excess) produced the expected reduction in fluorescence intensity and conclude that they successfully competed TNP-ATP off their protein. They further support this conclusion by showing that the relationship is linear. However, this interpretation is problematic because inspection of the spectra after ATP addition shows a clear λ_{em} blue shift of 16 nm, not the expected small red shift. Simple dilution of the sample (by ATP addition) could cause the intensity decrease, but dilution would not cause a shift in λ_{em}. What could cause a blue shift and a decrease in intensity? There is no clear answer, but some possible reasons follow. 1) Using 15 mM ATP may have caused a decrease in fluorescence and peak shift because of inner-filter effects from ATP absorption. The authors state that they corrected for inner-filter effects after adding TNP-ATP to their protein, but it is not clear whether this correction was also done after the addition of ATP. 2) The protein may have formed aggregates after ATP addition, which would scatter light, decreasing the intensity of light available for excitation and hence decreasing fluorescent emissions. Or 3) perhaps adding 15 mM ATP changed the pH beyond the buffering capacity of their solution, producing a spectrum similar to the dashed curves shown in Fig. 3 (which are blue shifted 11–14 nm).

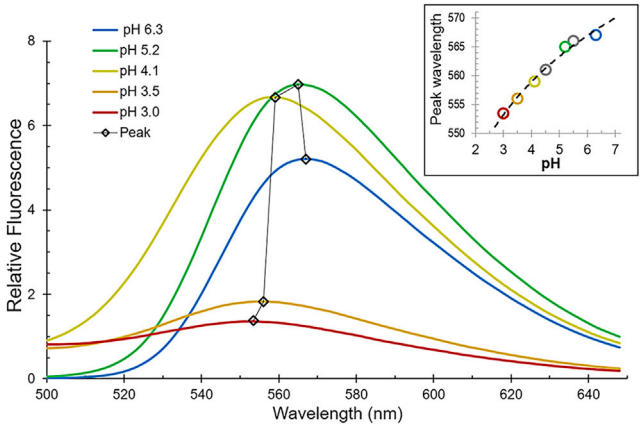

FIGURE 3 TNP-ATP fluorescence spectra are changed by pH. These previously unpublished spectra show that peak wavelength (and intensity) change with pH. TNP-ATP was added to buffer (150 mM KCl, 8 mM HEPES (pH 6.3)) and titrated with small additions of concentrated H_3PO_4. Peak wavelength was determined at each pH (spectra were not corrected for dilution). The black line indicates the order of additions from pH 6.3 (*blue line*) to pH 3.0 (*red line*). (*Inset*) Peak wavelength (λ_{em}) decreases monotonically with decreasing pH. Specifically, acidification from pH 6.3 to 3.5 caused a blue shift of 11 nm. $\lambda_{ex} = 410$ nm, excitation and emission slits = 5 nm.

Interference from other molecules

In the above examples, unexpected spectral changes were observed. Another problem is that of a false positive, in which there is a spectral change, but it is due to a component other than the one being tested. In example 3 below, an unexpected accessory protein in the assay may bind TNP-ATP and give a false positive TNP-ATP spectral signal. In example 4, it is shown that detergents, which are sometimes used with proteins (7,41,77,86), can produce signals typically ascribed to protein binding.

Example 3: interference from accessory proteins. Another issue with using TNP-ATP in ligand binding studies is that necessary accessory molecules may alter the environment of TNP-ATP or directly interact with TNP-ATP, giving a false positive signal of binding. A study by Yao and Hersh (144) claimed that insulin could not compete TNP-ATP out of the insulin-binding site of the protein insulin-degrading enzyme (IDE). Because insulin is a small protein that may directly interact with TNP-ATP, this apparent inability of insulin to compete with TNP-ATP may be because of an interaction of TNP-ATP with insulin rather than with IDE.

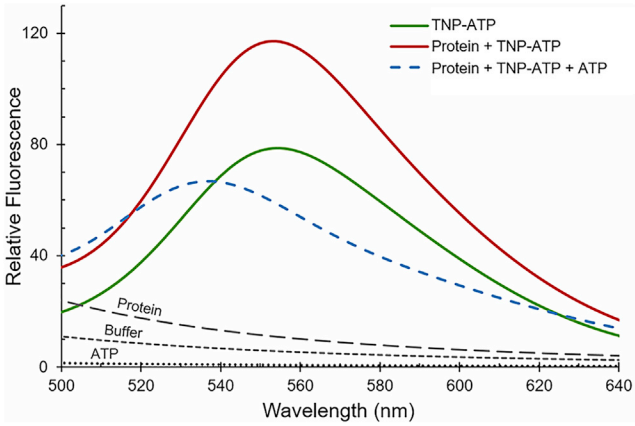

FIGURE 4 Lack of red shift after addition of ATP to TNP-ATP bound to protein. Fluorescence data are redrawn from Fig. 9 *A* in (143). The TNP-ATP spectrum (*green line*) changes after the addition of protein (P68 from *Antheraea mylitta*, *red line*) with an increase in intensity and a small (~2 nm) blue shift, consistent with TNP-ATP moving from an aqueous phase to the more hydrophobic ligand binding pocket. Subsequent addition of a 3000× excess of ATP decreases the fluorescence intensity (*blue dashed line*) and so appears to compete off the TNP-ATP; however, the spectrum does not return to the original TNP-ATP spectrum, but instead, the peak shifts 16 nm further to the left (blue shift). Possible reasons are given in the text, including solution acidification.

A study done by MacGregor et al. (145) illustrates this same point. Their study used phospholipids, especially PIP2 (phosphatidylinositol 4,5-bisphosphate), to examine the interactions of TNP-ATP with ATP-gated K+ channels. They observed an increase in fluorescence when TNP-ATP was added to their K+ channels, indicating binding. Subsequent addition of PIP2 (but not inositol trisphosphate) decreased fluorescence, which they interpret as TNP-ATP being displaced from the protein as PIP2 binds. In this study, the researchers' data suggested that small amounts of phospholipid were able to out-compete TNP-ATP for access to the binding site of an ATP-gated channel. A later report (146) showed the same result with just 39 amino acids from the COOH terminus of the protein. However, the control experiment of adding PIP2 to TNP-ATP in the absence of protein was not reported. This leaves open the alternate conclusion that TNP-ATP binds to PIP2. Although their findings might be suspect, this group did perform good controls: pretreating with PIP2, which abolished TNP-ATP binding; competing TNP-ATP off with MgATP (which reduced the enhanced fluorescence of TNP-ATP by 50–70%); and using a pulldown assay to verify that their results were not just a fluorescent artifact (145,146). However, the fact that TNP-ATP is highly sensitive to its surroundings still casts doubt on the researchers' interpretation with respect to ATP binding.

Consistent with lipids altering TNP-ATP fluorescence, a study of ATP binding to Annexin IV by Bandorowicz-Pikula et al. (147), observed a blue shift and an increase in TNP-ATP fluorescence when liposomes (asolectin/cholesterol 4:1 w/w) were added to their protein. Because annexin IV is a known lipid binding protein, this was interpreted in the context of lipid-protein interactions, but the results are also consistent with possible spectrum changes due to lipid-TNP-ATP interactions.

Example 4: interference from detergents. Because it is clear that the solvent environment changes the TNP-ATP fluorescence spectrum, it should not be surprising if lipids, surfactants, or detergents also alter the spectrum. This can be a concern, especially when the protein is embedded in a lipid membrane or when surfactants are used to solubilize or stabilize the protein of interest (e.g., (7,41,77,86)). The extent of this problem is clear in the simple experiment performed in our lab shown in Fig. 5. Here, the zwitterionic detergent, CHAPS, was added to a buffered, protein-free solution of TNP-ATP, causing both a 14× increase in fluorescence intensity and a blue shift of nearly 20 nm in peak wavelength; this exceeds most reported fluorescence changes after TNP-ATP binding to proteins. The concentration of CHAPS used (3.8 and 5.6 mM) is below the critical micelle concentration (= 6.5 mM) reported for CHAPS (148). It is especially surprising that after this change, the addition of a slight excess of pH-adjusted ATP (6.0 mM) nearly completely reversed the fluorescence increase and partly reversed the blue shift (Fig. 5). We have observed that other common detergents (i.e., Triton X-100, Tween 20, and SDS) also induced a similar fluorescence spectral change when added to TNP-ATP (data not shown).

Best practices

Despite these problems, the fluorescence probe TNP, when attached to nucleotides, remains an important tool for studying the interaction of nucleotides with proteins. To aid the potential future user of TNP-ATP, we refer the reader to two chapters that provide detailed protocols focused specifically on protein binding with TNP-ATP (8,9). Additionally, in this review, we have gathered and presented measured binding parameters and the conditions used for many of the diverse proteins studied with TNP-ATP. Although many reports are not free from alternate interpretations, we present below a summary of guidelines and precautions noted above that all users should consider so that the least ambiguous results are obtained.

1. When the fluorescence and absorption properties of TNP-ATP change upon binding to proteins, it is likely

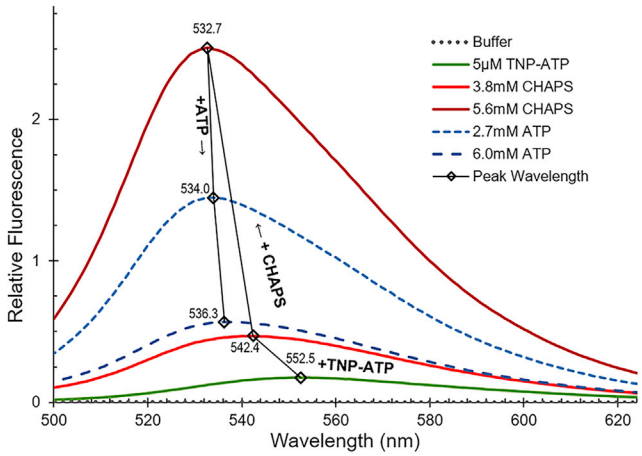

FIGURE 5 Previously unpublished data showing that at pH 7, the detergent CHAPS produces TNP-ATP spectral changes indistinguishable from many ATP binding proteins. In this case, adding CHAPS (5.6 mM) to TNP-ATP (5 μM, *green line*) caused a 14× increase in intensity and a ~20 nm blue shift (552.5–532.7 nm) in λ_{em} (*dark red line*). Addition of a slight excess (6 mM) of ATP (titrated to pH 7) decreased the intensity by 83% and caused a red shift of ~4 nm (*dashed blue line*). The black line indicates the order of additions, which caused a 20% overall dilution. λ_{ex} = 410 nm, excitation and emission slits = 5 nm.

due to the change in polarity of the environment surrounding TNP. However, spectral changes can also be due to the following:

   a. Changes in solvent, for example, adding ethanol, dimethylformamide, or glycerol (11–13).
   b. Changes in pH (4,10–12) as in Figs. 1 and 3. Therefore, the pH of all solutions should be checked before addition to the sample, especially concentrated solutions of ATP (54).
   c. Changes in viscosity (12).
   d. Changes in salt (140).
   e. Additions of lipids or detergents (see Example 3: interference from accessory proteins and Example 4: interference from detergents).

2. Binding increases fluorescent intensity and causes a blue shift in peak wavelength. The blue shift is less susceptible to artifacts that alter apparent changes in intensity (see Unexpected spectral changes).
3. TNP typically increases nucleotide binding by 20–2000 times. This high affinity allows the use of simplified equations to calculate K_d (64,65).
4. There may be more than one binding site with similar or different affinities (e.g., CheA (27,28). Nonspecific binding is also possible (95,118).
5. TNP-ATP is hydrolyzed normally by some proteins (e.g., CpABC4 and the F_1-ATPase) or at a reduced rate (e.g., hexokinase and PTK) and not at all by others (e.g., CheA, and PC).
6. Additional techniques are needed to confirm binding (e.g., using radiolabeled TNP-[γ^{32}]ATP (86); see also Other methods to confirm TNP-ATP binding data). Normally, specific binding could be confirmed by competing off TNP-ATP with ATP; however, the high affinity of TNP-ATP usually prevents this, even at high doses of ATP (an exception is the protein CDKA;1 (75)).

Recent uses of TNP-ATP

TNP-ATP continues to be a useful research tool. A search on PubMed and Web of Science for the years 2019–2020 shows dozens of works in which TNP-ATP was used to study ATP-interacting proteins, using both its fluorescence and its characteristic high affinity. Some of these were discussed above; additional examples listed below show the clever and diverse ways TNP-ATP is being used:

1. Determining K_d (or $K_{0.5}$) for multiple nucleotides (i.e., ATP, ADP, AMP, and TNP-ATP) with several known nucleotide binding proteins, including VNUT (see Table 1) (47), ABCF3 (see Table 4) (74), and ABCA4 (149).
2. Determining differences in binding of TNP-ATP to wild-type and mutant proteins including Rad51 (a human DNA binding protein (150)), SaUspA (a stress-sensing protein from *Sulfolobus acidocaldarius*, see Table 4 (79)), and Cek1 (a MAP kinase from *Candida albicans* (151)).
3. Checking ATP binding to a known ATP binding protein after phosphorylation or dephosphorylation of a serine in the binding pocket (152).
4. Testing for possible ATP binding to a hypothetical protein from an open reading frame—Alr0765 from *Anabaena* (115).
5. Using TNP (and other moieties) attached to ATP to explore ribonucleotide binding to a polymerase with and without point mutations (153).
6. As a FRET pair to measure interaction and distances between binding sites in the ATP-sensitive K+ channel (Kir6.2, see Table 4) (26,80).
7. As a fluorescence marker to observe compartment localization of ATP in a study of artificial protocell organization (154) and of membrane-free organelles (155).
8. As an antagonist of the P2X receptor (specifically of the P2X1, P2X2, P2X3, and P2X7 receptors) as reviewed in (156). In addition, the x-ray structure of P2X3 complexed with TNP-ATP was used in a study aimed at development of a P2X3 blocker (157).

Conclusions

Since its first synthesis and use 50 years ago (1,4), TNP-ATP has been used in hundreds of studies and

has been a highly useful molecule for studying the binding of ATP to proteins. Like Janus, the ancient mythological god with two faces, TNP-ATP also has two faces, ATP and TNP, that imbue it with both power and problems. Its power comes from both parts, it can masquerade as ATP and bind to proteins in their ATP binding pockets, and through its TNP face it can reveal to the careful scientist the extent and nature of that binding through changes in TNP fluorescence. Unfortunately, the properties of TNP not only allow it to fluoresce but also alter the nature of binding, requiring caution in interpreting binding results.

We have reviewed how TNP-ATP fluorescence is highly sensitive to its environment, altering its spectral properties because of changes in polarity and viscosity that take place when it enters the hydrophobic binding pocket of a protein. Typically, when TNP-ATP moves from an aqueous environment to the more hydrophobic binding pocket of an ATP binding protein, the fluorescence intensity increases severalfold and the peak fluorescence (λ_{em}) is blue shifted 4–15 nm (Tables 1, 2, 3, and 4). These characteristics have led researchers to use TNP-ATP to understand how ATP binds to proteins. Researchers have also used more specialized techniques such as x-ray crystallography and molecular modeling and docking to understand the shape and hydrophobicity of protein binding pockets (48,54–56,61,63,78,83,119,158).

Because of these spectral changes, TNP-ATP has been used to measure the binding constants, rate constants, and rates of ATP hydrolysis for many different proteins. In many cases, it has been shown that the K_d of binding for TNP-ATP is 20–2000× higher than for ATP, but there are also examples for which the K_d is similar (Table 3). Sometimes TNP-ATP acts as an inhibitor of ATP binding, and K_i or IC50 values have been determined (Table 4).

Although TNP-ATP is highly useful in studying ATP binding sites, its use comes with several caveats: 1) it often binds with much higher affinity than ATP, 2) it is not hydrolyzable by some kinases, 3) unexpected spectral changes can occur (e.g., because of inner-filter effects, formation of precipitates, protein structural changes after binding, and pH changes), and 4) other molecules can interfere with its fluorescence. Examples of some of these problems were discussed and are shown in Figs. 3, 4, and 5. One particularly worrisome problem is that detergents can interact with TNP-ATP in a manner indistinguishable from its interaction with ATP binding proteins (Fig. 5). The best results are most likely when the factors presented in the Best practices section are followed. These factors should be taken into consideration when planning any experiment involving TNP-ATP or other TNP nucleotides.

On the other hand, TNP-ATP does shine as a useful probe with few problems in several other applications. Examples for which there are fewer complications with using TNP-ATP include fluorescence microscopy and FRET. TNP-ATP can also be useful in binding studies in which different TNP nucleotides are compared to each other, e.g., comparing the K_d of TNP-ATP to the K_d of TNP-ADP and TNP-AMP.

The limitations to using TNP-ATP for binding studies mean that careful controls and alternate methods need to be used if results with TNP-ATP are to be correctly interpreted with respect to how ATP binds to proteins. More work using x-ray crystallography would be useful to understand exactly how TNP-ATP binds to the binding pockets of various proteins. Additionally, it will always be important to see under what conditions TNP-ATP can be completely competed out of a protein binding site by ATP. Few of the experiments reviewed here provided convincing evidence that ATP addition can fully displace TNP-ATP, as would be shown by a complete return to both the fluorescence intensity and peak wavelength exhibited by TNP-ATP in solution before the addition of protein. It is hoped that future research using TNP-ATP will become even more powerful through understanding the limitations as well as the potential of TNP-ATP as a probe of ATP binding sites.

AUTHOR CONTRIBUTIONS

D.J.W. wrote the manuscript, prepared figures and tables, and analyzed and interpreted data. E.C.W. ran experiments and wrote the manuscript. R.E.C. ran experiments, prepared figures and tables, and edited the manuscript. All authors read and approved the final manuscript.

ACKNOWLEDGMENTS

We are grateful for the many undergraduate students who through the years have helped with fluorescence measurement in our laboratory. We are especially thankful to Ani C. Nichol and Wade J. Whitt, who ran key experiments, and to Keith Menser, who helped prepare an initial draft of the tables. We thank Dr. David Busath for providing valuable feedback on the manuscript. This work was supported by Brigham Young University.

DECLARATION OF INTERESTS

All authors declare they have no conflict of interest.

REFERENCES

1. Azegami, M., and K. Iwai. 1964. Specific modification of nucleic acids and their constituents with trinitrophenyl group. *J. Biochem.* 55:346–348.
2. Hiratsuka, T. 1975. 2′ (or 3′)-O-(2, 4, 6-trinitrophenyl)adenosine 5′-triphosphate as a probe for the binding site of heavy meromyosin ATPase. *J. Biochem.* 78:1135–1147.

3. Hiratsuka, T. 2003. Fluorescent and colored trinitrophenylated analogs of ATP and GTP. *Eur. J. Biochem.* 270:3479–3485.
4. Hiratsuka, T., and K. Uchida. 1973. Preparation and properties of 2′(or 3′)-O-(2,4,6-trinitrophenyl) adenosine 5′-triphosphate, an analog of adenosine triphosphate. *Biochim. Biophys. Acta.* 320:635–647.
5. Grubmeyer, C., and H. S. Penefsky. 1981. The presence of two hydrolytic sites on beef heart mitochondrial adenosine triphosphatase. *J. Biol. Chem.* 256:3718–3727.
6. Dupont, Y., Y. Chapron, and R. Pougeois. 1982. Titration of the nucleotide binding sites of sarcoplasmic reticulum Ca2+ -ATPase with 2′,3′-O-(2,4,6-trinitrophenyl) adenosine 5′-triphosphate and 5′-diphosphate. *Biochem. Biophys. Res. Commun.* 106:1272–1279.
7. Berman, M. C. 1986. Absorbance and fluorescence properties of 2′(3′)-O-(2,4,6-trinitrophenyl)adenosine 5′-triphosphate bound to coupled and uncoupled Ca2+-ATPase of skeletal muscle sarcoplasmic reticulum. *J. Biol. Chem.* 261:16494–16501.
8. LaConte, L. E. W., S. Srivastava, and K. Mukherjee. 2017. Probing protein kinase-ATP interactions using a fluorescent ATP analog. *Methods Mol. Biol.* 1647:171–183.
9. Hindie, V., L. A. Lopez-Garcia, and R. M. Biondi. 2012. Use of a fluorescent ATP analog to probe the allosteric conformational change in the active site of the protein kinase PDK1. *Methods Mol. Biol.* 928:133–141.
10. Murataliev, M. B. 1995. Interaction of mitochondrial F1-ATPase with trinitrophenyl derivatives of ATP. Photoaffinity labeling of binding sites with 2-azido-2′,3′-O-(4,6-trinitrophenyl)adenosine 5′-triphosphate. *Eur. J. Biochem.* 232:578–585.
11. Ye, J. Y., M. Yamauchi, …, M. Ishikawa. 1999. Spectroscopic properties of 2′-(or-3′)-O-(2,4,6-trinitrophenyl) adenosine 5′-triphosphate revealed by time-resolved fluorescence spectroscopy. *J. Phys. Chem. B.* 103:2812–2817.
12. Moczydlowski, E. G., and P. A. Fortes. 1981. Characterization of 2′,3′-O-(2,4,6-trinitrocyclohexadienylidine)adenosine 5′-triphosphate as a fluorescent probe of the ATP site of sodium and potassium transport adenosine triphosphatase. Determination of nucleotide binding stoichiometry and ion-induced changes in affinity for ATP. *J. Biol. Chem.* 256:2346–2356.
13. Hiratsuka, T. 1982. Biological activities and spectroscopic properties of chromophoric and fluorescent analogs of adenine nucleoside and nucleotides, 2′,3′-O-(2,4,6-trinitrocyclohexadienylidene) adenosine derivatives. *Biochim. Biophys. Acta.* 719:509–517.
14. Ko, Y. H., P. J. Thomas, …, P. L. Pedersen. 1993. The cystic fibrosis transmembrane conductance regulator. Overexpression, purification, and characterization of wild type and delta F508 mutant forms of the first nucleotide binding fold in fusion with the maltose-binding protein. *J. Biol. Chem.* 268:24330–24338.
15. Mockett, B. G., G. D. Housley, and P. R. Thorne. 1994. Fluorescence imaging of extracellular purinergic receptor sites and putative ecto-ATPase sites on isolated cochlear hair cells. *J. Neurosci.* 14:6992–7007.
16. Mironov, S. L. 2007. ADP regulates movements of mitochondria in neurons. *Biophys. J.* 92:2944–2952.
17. Nowodworska, A., A. M. J. M. van den Maagdenberg, …, E. Fabbretti. 2017. In situ imaging reveals properties of purinergic signalling in trigeminal sensory ganglia in vitro. *Purinergic Signal.* 13:511–520.
18. Faria, R. X., H. R. Freitas, and R. A. M. Reis. 2017. P2X7 receptor large pore signaling in avian Müller glial cells. *J. Bioenerg. Biomembr.* 49:215–229.
19. Lee, N. Y., and J. G. Koland. 2005. Conformational changes accompany phosphorylation of the epidermal growth factor receptor C-terminal domain. *Protein Sci.* 14:2793–2803.
20. Logvinova, D. S., A. M. Matyushenko, …, D. I. Levitsky. 2018. Transient interaction between the N-terminal extension of the essential light chain-1 and motor domain of the myosin head during the ATPase cycle. *Biochem. Biophys. Res. Commun.* 495:163–167.
21. Chen, B., J. E. Mahaney, …, T. C. Squier. 2008. Concerted but noncooperative activation of nucleotide and actuator domains of the Ca-ATPase upon calcium binding. *Biochemistry.* 47:12448–12456.
22. Yamada, K., and S. Fujita. 1998. Communications between the nucleotide- and actin-binding site of the myosin head in muscle fibers. *Adv. Exp. Med. Biol.* 453:419–423.
23. Miki, M., T. Miura, …, Y. Maéda. 1998. Fluorescence resonance energy transfer between points on tropomyosin and actin in skeletal muscle thin filaments: does tropomyosin move? *J. Biochem.* 123:1104–1111.
24. Divita, G., R. S. Goody, …, A. Di Pietro. 1993. Structural mapping of catalytic site with respect to alpha-subunit and noncatalytic site in yeast mitochondrial F1-ATPase using fluorescence resonance energy transfer. *J. Biol. Chem.* 268:13178–13186.
25. Shapiro, A. B., K. D. Gibson, …, R. E. McCarty. 1991. Fluorescence resonance energy transfer mapping of the fourth of six nucleotide-binding sites of chloroplast coupling factor 1. *J. Biol. Chem.* 266:17276–17285.
26. Usher, S. G., F. M. Ashcroft, and M. C. Puljung. 2020. Nucleotide inhibition of the pancreatic ATP-sensitive K+ channel explored with patch-clamp fluorometry. *Elife.* 9:e52775.
27. Eaton, A. K., and R. C. Stewart. 2009. The two active sites of Thermotoga maritima CheA dimers bind ATP with dramatically different affinities. *Biochemistry.* 48:6412–6422.
28. Eaton, A. K., and R. C. Stewart. 2010. Kinetics of ATP and TNP-ATP binding to the active site of CheA from Thermotoga maritima. *Biochemistry.* 49:5799–5809.
29. Cheng, K., and J. G. Koland. 1996. Nucleotide binding by the epidermal growth factor receptor protein-tyrosine kinase. Trinitrophenyl-ATP as a spectroscopic probe. *J. Biol. Chem.* 271:311–318.
30. Voynova, N. E., Z. Fu, …, H. M. Miziorko. 2008. Human mevalonate diphosphate decarboxylase: characterization, investigation of the mevalonate diphosphate binding site, and crystal structure. *Arch. Biochem. Biophys.* 480:58–67.
31. Krepkiy, D., and H. M. Miziorko. 2004. Identification of active site residues in mevalonate diphosphate decarboxylase: implications for a family of phosphotransferases. *Protein Sci.* 13:1875–1881.
32. Preobrazhenskaya, Y. V., A. I. Stenko, …, V. Y. Lugovtsev. 2013. Binding stoichiometry of a recombinant selenophosphate synthetase with one synonymic substitution E197D to a fluorescent nucleotide analog of ATP, TNP-ATP. *J. Amino Acids.* 2013:983565.
33. Preabrazhenskaya, Y. V., I. Y. Kim, and T. C. Stadtman. 2009. Binding of ATP and its derivatives to selenophosphate synthetase from *Escherichia coli*. *Biochemistry (Mosc.).* 74:910–916.
34. Adina-Zada, A., R. Hazra, …, P. V. Attwood. 2011. Probing the allosteric activation of pyruvate carboxylase using 2′,3′-O-(2,4,6-trinitrophenyl) adenosine 5′-triphosphate as a fluorescent mimic of the allosteric activator acetyl CoA. *Arch. Biochem. Biophys.* 509:117–126.
35. Peters, B. A., and K. E. Neet. 1978. Yeast hexokinase PII. Conformational changes induced by substrates and substrate analogues. *J. Biol. Chem.* 253:6826–6831.
36. Arora, K. K., P. Shenbagamurthi, …, P. L. Pedersen. 1990. Glucose phosphorylation. Interaction of a 50-amino acid peptide of yeast hexokinase with trinitrophenyl ATP. *J. Biol. Chem.* 265:5324–5328.
37. Grossman, J. D., K. A. Gay, …, D. L. Perlstein. 2019. Coupling nucleotide binding and hydrolysis to iron-sulfur cluster

acquisition and transfer revealed through genetic dissection of the Nbp35 ATPase site. *Biochemistry.* 58:2017–2027.

38. Hormaeche, I., I. Alkorta, …, F. De La Cruz. 2002. Purification and properties of TrwB, a hexameric, ATP-binding integral membrane protein essential for R388 plasmid conjugation. *J. Biol. Chem.* 277:46456–46462.
39. Rai, V., S. Shukla, …, R. Prasad. 2005. Functional characterization of N-terminal nucleotide binding domain (NBD-1) of a major ABC drug transporter Cdr1p of Candida albicans: uncommon but conserved Trp326 of Walker B is important for ATP binding. *Biochemistry.* 44:6650–6661.
40. Jha, S., N. Karnani, …, R. Prasad. 2003. Purification and characterization of the N-terminal nucleotide binding domain of an ABC drug transporter of Candida albicans: uncommon cysteine 193 of Walker A is critical for ATP hydrolysis. *Biochemistry.* 42:10822–10832.
41. Benitez, A. J., M. J. Arrowood, and J. R. Mead. 2009. Functional characterization of the nucleotide binding domain of the Cryptosporidium parvum CpABC4 transporter: an iron-sulfur cluster transporter homolog. *Mol. Biochem. Parasitol.* 165:103–110.
42. Kidd, J. F., M. Ramjeesingh, …, C. E. Bear. 2004. A heteromeric complex of the two nucleotide binding domains of cystic fibrosis transmembrane conductance regulator (CFTR) mediates ATPase activity. *J. Biol. Chem.* 279:41664–41669.
43. Stratford, F. L. L., M. Ramjeesingh, …, C. E. Bear. 2007. The Walker B motif of the second nucleotide-binding domain (NBD2) of CFTR plays a key role in ATPase activity by the NBD1-NBD2 heterodimer. *Biochem. J.* 401:581–586.
44. Randak, C., P. Neth, …, W. Machleidt. 1997. A recombinant polypeptide model of the second nucleotide-binding fold of the cystic fibrosis transmembrane conductance regulator functions as an active ATPase, GTPase and adenylate kinase. *FEBS Lett.* 410:180–186.
45. Vergani, P., C. Basso, …, D. C. Gadsby. 2005. Control of the CFTR channel's gates. *Biochem. Soc. Trans.* 33:1003–1007.
46. Ko, Y. H., P. J. Thomas, and P. L. Pedersen. 1994. The cystic fibrosis transmembrane conductance regulator. Nucleotide binding to a synthetic peptide segment from the second predicted nucleotide binding fold. *J. Biol. Chem.* 269:14584–14588.
47. Iwai, Y., S. Kamatani, …, H. Omote. 2019. Function of essential chloride and arginine residue in nucleotide binding to vesicular nucleotide transporter. *J. Biochem.* 165:479–486.
48. Grycova, L., Z. Lansky, …, J. Teisinger. 2007. ATP binding site on the C-terminus of the vanilloid receptor. *Arch. Biochem. Biophys.* 465:389–398.
49. Bishop, J. E., J. D. Johnson, and M. C. Berman. 1984. Transient kinetic analysis of turnover-dependent fluorescence of 2′,3′-O-(2,4,6-trinitrophenyl)-ATP bound to Ca2+-ATPase of sarcoplasmic reticulum. *J. Biol. Chem.* 259:15163–15171.
50. Dupont, Y., R. Pougeois, …, S. Verjovsky-Almeida. 1985. Two distinct classes of nucleotide binding sites in sarcoplasmic reticulum Ca-ATPase revealed by 2′,3′-O-(2,4,6-trinitrocyclohexadienylidene)-ATP. *J. Biol. Chem.* 260:7241–7249.
51. Carvalho-Alves, P. C., V. R. Hering, …, S. Verjovski-Almeida. 2000. Requirement of the hinge domain for dimerization of Ca2+-ATPase large cytoplasmic portion expressed in bacteria. *Biochim. Biophys. Acta.* 1467:73–84.
52. Faller, L. D. 1990. Binding of the fluorescent substrate analogue 2′,3′-O-(2,4,6-trinitrophenylcyclohexadienylidene)adenosine 5′-triphosphate to the gastric H+,K(+)-ATPase: evidence for cofactor-induced conformational changes in the enzyme. *Biochemistry.* 29:3179–3186.
53. Faller, L. D. 1989. Competitive binding of ATP and the fluorescent substrate analogue 2′,3′-O-(2,4,6-trinitrophenylcyclohexadienylidine) adenosine 5′-triphosphate to the gastric H+,K+-ATPase: evidence for two classes of nucleotide sites. *Biochemistry.* 28:6771–6778.
54. Kubala, M., K. Hofbauerová, …, E. Amler. 2002. Phe(475) and Glu(446) but not Ser(445) participate in ATP-binding to the alpha-subunit of Na(+)/K(+)-ATPase. *Biochem. Biophys. Res. Commun.* 297:154–159.
55. Lánský, Z., M. Kubala, …, E. Amler. 2004. The hydrogen bonds between Arg423 and Glu472 and other key residues, Asp443, Ser477, and Pro489, are responsible for the formation and a different positioning of TNP-ATP and ATP within the nucleotide-binding site of Na(+)/K(+)-ATPase. *Biochemistry.* 43:8303–8311.
56. Krumscheid, R., R. Ettrich, …, W. Schoner. 2004. The phosphatase activity of the isolated H4-H5 loop of Na+/K+ ATPase resides outside its ATP binding site. *Eur. J. Biochem.* 271:3923–3936.
57. Capieaux, E., C. Rapin, …, A. Goffeau. 1993. Overexpression in *Escherichia coli* and purification of an ATP-binding peptide from the yeast plasma membrane H(+)-ATPase. *J. Biol. Chem.* 268:21895–21900.
58. Grubmeyer, C., and H. S. Penefsky. 1981. Cooperatively between catalytic sites in the mechanism of action of beef heart mitochondrial adenosine triphosphatase. *J. Biol. Chem.* 256:3728–3734.
59. Hisabori, T., E. Muneyuki, …, M. Yoshida. 1992. Single site hydrolysis of 2′,3′-O-(2,4,6-trinitrophenyl)-ATP by the F1-ATPase from thermophilic bacterium PS3 is accelerated by the chase-addition of excess ATP. *J. Biol. Chem.* 267:4551–4556.
60. Murataliev, M. B., and P. D. Boyer. 1994. Interaction of mitochondrial F1-ATPase with trinitrophenyl derivatives of ATP and ADP. Participation of third catalytic site and role of Mg2+ in enzyme inactivation. *J. Biol. Chem.* 269:15431–15439.
61. Mao, H. Z., and J. Weber. 2007. Identification of the betaTP site in the x-ray structure of F1-ATPase as the high-affinity catalytic site. *Proc. Natl. Acad. Sci. USA.* 104:18478–18483.
62. Weber, J., and A. E. Senior. 2004. Fluorescent probes applied to catalytic cooperativity in ATP synthase. *In* Methods in Enzymology, *Volume 380*. J. M. Holt, M. L. Johnson, and G. K. Ackers, eds.. Academic Press, pp. 132–152.
63. Zhao, J. H., K. Beyrakhova, …, J. L. Rubinstein. 2017. Molecular basis for the binding and modulation of V-ATPase by a bacterial effector protein. *PLoS Pathog.* 13:e1006394.
64. Kubala, M., J. Plásek, and E. Amler. 2004. Fluorescence competition assay for the assessment of ATP binding to an isolated domain of Na+, K(+)-ATPase. *Physiol. Res.* 53:109–113.
65. Kubala, M., J. Plásek, and E. Amler. 2003. Limitations in linearized analyses of binding equilibria: binding of TNP-ATP to the H4-H5 loop of Na/K-ATPase. *Eur. Biophys. J.* 32:363–369.
66. Stewart, R. C., R. VanBruggen, …, A. J. Wolfe. 1998. TNP-ATP and TNP-ADP as probes of the nucleotide binding site of CheA, the histidine protein kinase in the chemotaxis signal transduction pathway of *Escherichia coli*. *Biochemistry.* 37:12269–12279.
67. Bilwes, A. M., C. M. Quezada, …, M. I. Simon. 2001. Nucleotide binding by the histidine kinase CheA. *Nat. Struct. Biol.* 8:353–360.
68. Ripoll-Rozada, J., Y. García-Cazorla, …, I. Arechaga. 2016. Type IV traffic ATPase TrwD as molecular target to inhibit bacterial conjugation. *Mol. Microbiol.* 100:912–921.
69. Ripoll-Rozada, J., A. Peña, …, I. Arechaga. 2012. Regulation of the type IV secretion ATPase TrwD by magnesium: implications for catalytic mechanism of the secretion ATPase superfamily. *J. Biol. Chem.* 287:17408–17414.
70. Cloherty, E. K., K. B. Levine, …, A. Carruthers. 2002. Cooperative nucleotide binding to the human erythrocyte sugar transporter. *Biochemistry.* 41:12639–12651.
71. Lucius, A. L., M. J. Jezewska, and W. Bujalowski. 2006. The *Escherichia coli* PriA helicase has two nucleotide-binding sites differing dramatically in their affinities for nucleotide cofactors.

1. Intrinsic affinities, cooperativities, and base specificity of nucleotide cofactor binding. *Biochemistry.* 45:7202–7216.

72. Lucius, A. L., M. J. Jezewska, …, W. Bujalowski. 2006. Kinetic mechanisms of the nucleotide cofactor binding to the strong and weak nucleotide-binding site of the *Escherichia coli* PriA helicase. 2. *Biochemistry.* 45:7217–7236.

73. Andreeva, I. E., A. Roychowdhury, …, W. Bujalowski. 2009. Mechanisms of interactions of the nucleotide cofactor with the RepA protein of plasmid RSF1010. Binding dynamics studied using the fluorescence stopped-flow method. *Biochemistry.* 48:10620–10636.

74. Peterson, E., E. Shippee, …, P. Kaur. 2019. Biochemical characterization of the mouse ABCF3 protein, a partner of the flavivirus-resistance protein OAS1B. *J. Biol. Chem.* 294:14937–14952.

75. Méndez, A. A. E., I. C. Mangialavori, …, S. M. Gallego. 2020. Tyr-nitration in maize CDKA;1 results in lower affinity for ATP binding. *Biochim. Biophys. Acta. Proteins Proteom.* 1868:140479.

76. Flörke, H., F. P. Thinnes, …, N. Hilschmann. 1994. Channel active mammalian porin, purified from crude membrane fractions of human B lymphocytes and bovine skeletal muscle, reversibly binds adenosine triphosphate (ATP). *Biol. Chem. Hoppe Seyler.* 375:513–520.

77. Lawton, P., M. Pélandakis, …, N. Walchshofer. 2007. Overexpression, purification and characterization of a hexahistidine-tagged recombinant extended nucleotide-binding domain 1 (NBD1) of the Cryptosporidium parvum CpABC3 for rational drug design. *Mol. Biochem. Parasitol.* 152:101–107.

78. Suryanarayana, S., M. Göttle, …, R. Seifert. 2009. Differential inhibition of various adenylyl cyclase isoforms and soluble guanylyl cyclase by 2′,3′-O-(2,4,6-trinitrophenyl)-substituted nucleoside 5′-triphosphates. *J. Pharmacol. Exp. Ther.* 330:687–695.

79. Ye, X., C. van der Does, and S. V. Albers. 2020. *Sa*UspA, the universal stress protein of *Sulfolobus acidocaldarius* stimulates the activity of the PP2A phosphatase and is involved in growth at high salinity. *Front. Microbiol.* 11:598821.

80. Puljung, M., N. Vedovato, …, F. Ashcroft. 2019. Activation mechanism of ATP-sensitive K+ channels explored with real-time nucleotide binding. *Elife.* 8:e41103.

81. Wang, X. L., T. Lu, …, H. C. Lee. 2006. Inhibition of ATP binding to the carboxyl terminus of Kir6.2 by epoxyeicosatrienoic acids. *Biochim. Biophys. Acta.* 1761:1041–1049.

82. Rivas, S., S. Bolland, …, F. de la Cruz. 1997. TrwD, a protein encoded by the IncW plasmid R388, displays an ATP hydrolase activity essential for bacterial conjugation. *J. Biol. Chem.* 272:25583–25590.

83. Han, X., Y. Huang, …, J. Wan. 2016. New insight into the binding modes of TNP-AMP to human liver fructose-1,6-bisphosphatase. *Spectrochim. Acta A Mol. Biomol. Spectrosc.* 165:155–160.

84. Nelson, S. W., J. Y. Choe, …, H. J. Fromm. 2000. Mutations in the hinge of a dynamic loop broadly influence functional properties of fructose-1,6-bisphosphatase. *J. Biol. Chem.* 275:29986–29992.

85. Mancl, J. M., W. P. Black, …, F. D. Schubot. 2016. Crystal structure of a type IV pilus assembly ATPase: insights into the molecular mechanism of PilB from Thermus thermophilus. *Structure.* 24:1886–1897.

86. Watanabe, T., and G. Inesi. 1982. The use of 2′,3′-O-(2,4,6-trinitrophenyl) adenosine 5′-triphosphate for studies of nucleotide interaction with sarcoplasmic reticulum vesicles. *J. Biol. Chem.* 257:11510–11516.

87. DeJesus, F., J. L. Girardet, and Y. Dupont. 1993. Characterisation of ATP binding inhibition to the sarcoplasmic reticulum Ca(2+)-ATPase by thapsigargin. *FEBS Lett.* 332:229–232.

88. Davidson, G. A., and M. C. Berman. 1987. Phosphoenzyme conformational states and nucleotide-binding site hydrophobicity following thiol modification of the Ca2+-ATPase of sarcoplasmic reticulum from skeletal muscle. *J. Biol. Chem.* 262:7041–7046.

89. McIntosh, D. B., and D. G. Woolley. 1994. Catalysis of an ATP analogue untethered and tethered to lysine 492 of sarcoplasmic reticulum Ca(2+)-ATPase. *J. Biol. Chem.* 269:21587–21595.

90. Berman, M. C., and S. J. Karlish. 2003. Interaction of an aromatic dibromoisothiouronium derivative with the Ca(2+)-ATPase of skeletal muscle sarcoplasmic reticulum. *Biochemistry.* 42:3556–3566.

91. Danko, S., K. Yamasaki, …, H. Suzuki. 2004. Distinct natures of beryllium fluoride-bound, aluminum fluoride-bound, and magnesium fluoride-bound stable analogues of an ADP-insensitive phosphoenzyme intermediate of sarcoplasmic reticulum Ca2+-ATPase: changes in catalytic and transport sites during phosphoenzyme hydrolysis. *J. Biol. Chem.* 279:14991–14998.

92. Danko, S., T. Daiho, …, H. Suzuki. 2009. Formation of the stable structural analog of ADP-sensitive phosphoenzyme of Ca2+-ATPase with occluded Ca2+ by beryllium fluoride: structural changes during phosphorylation and isomerization. *J. Biol. Chem.* 284:22722–22735.

93. Toyoshima, C., S. Yonekura, …, S. Iwasawa. 2011. Trinitrophenyl derivatives bind differently from parent adenine nucleotides to Ca2+-ATPase in the absence of Ca2+. *Proc. Natl. Acad. Sci. USA.* 108:1833–1838.

94. Moutin, M. J., M. Cuillel, …, Y. Dupont. 1994. Measurements of ATP binding on the large cytoplasmic loop of the sarcoplasmic reticulum Ca(2+)-ATPase overexpressed in *Escherichia coli*. *J. Biol. Chem.* 269:11147–11154.

95. Pratap, P. R., E. H. Hellen, …, J. D. Robinson. 1997. Transient kinetics of substrate binding to Na+/K(+)-ATPase measured by fluorescence quenching. *Biophys. Chem.* 69:137–151.

96. Moczydlowski, E. G., and P. A. Fortes. 1981. Inhibition of sodium and potassium adenosine triphosphatase by 2′,3′-O-(2,4,6-trinitrocyclohexadienylidene) adenine nucleotides. Implications for the structure and mechanism of the Na:K pump. *J. Biol. Chem.* 256:2357–2366.

97. Almeida, W. I., O. B. Martins, and P. C. Carvalho-Alves. 2006. Self-association of isolated large cytoplasmic domain of plasma membrane H+ -ATPase from *Saccharomyces cerevisiae*: role of the phosphorylation domain in a general dimeric model for P-ATPases. *Biochim. Biophys. Acta.* 1758:1768–1776.

98. Lee, J. H., D. N. Garboczi, …, P. L. Pedersen. 1990. Mitochondrial ATP synthase. cDNA cloning, amino acid sequence, overexpression, and properties of the rat liver alpha subunit. *J. Biol. Chem.* 265:4664–4669.

99. Weber, J., and A. E. Senior. 1997. Binding of TNP-ATP and TNP-ADP to the non-catalytic sites of *Escherichia coli* F1-ATPase. *FEBS Lett.* 412:169–172.

100. Dunn, S. D., and M. Futai. 1980. Reconstitution of a functional coupling factor from the isolated subunits of *Escherichia coli* F1 ATPase. *J. Biol. Chem.* 255:113–118.

101. Garboczi, D. N., P. J. Thomas, and P. L. Pedersen. 1990. Rat liver mitochondrial ATP synthase. Effects of mutations in the glycine-rich region of a beta subunit peptide on its interaction with adenine nucleotides. *J. Biol. Chem.* 265:14632–14637.

102. Garboczi, D. N., J. H. Hullihen, and P. L. Pedersen. 1988. Mitochondrial ATP synthase. Overexpression in *Escherichia coli* of a rat liver beta subunit peptide and its interaction with adenine nucleotides. *J. Biol. Chem.* 263:15694–15698.

103. Hong, S., and P. L. Pedersen. 2008. ATP synthase and the actions of inhibitors utilized to study its roles in human health, disease, and other scientific areas. *Microbiol. Mol. Biol. Rev.* 72:590–641.

104. Gresser, M. J., J. A. Myers, and P. D. Boyer. 1982. Catalytic site cooperativity of beef heart mitochondrial F1 adenosine

triphosphatase. Correlations of initial velocity, bound intermediate, and oxygen exchange measurements with an alternating three-site model. *J. Biol. Chem.* 257:12030–12038.

105. Cross, R. L., C. Grubmeyer, and H. S. Penefsky. 1982. Mechanism of ATP hydrolysis by beef heart mitochondrial ATPase. Rate enhancements resulting from cooperative interactions between multiple catalytic sites. *J. Biol. Chem.* 257:12101–12105.

106. Grubmeyer, C., R. L. Cross, and H. S. Penefsky. 1982. Mechanism of ATP hydrolysis by beef heart mitochondrial ATPase. Rate constants for elementary steps in catalysis at a single site. *J. Biol. Chem.* 257:12092–12100.

107. Paige, C., G. B. Maruthy, …, T. Price. 2018. Spinal inhibition of P2XR or p38 signaling disrupts hyperalgesic priming in male, but not female, mice. *Neuroscience.* 385:133–142.

108. Lambertucci, C., D. Dal Ben, …, R. Volpini. 2015. Medicinal chemistry of P2X receptors: agonists and orthosteric antagonists. *Curr. Med. Chem.* 22:915–928.

109. Pasqualetto, G., A. Brancale, and M. T. Young. 2018. The molecular determinants of small-molecule ligand binding at P2X receptors. *Front. Pharmacol.* 9:58.

110. Silva-Ramos, M., I. Silva, …, P. Correia-de-Sá. 2020. Activation of prejunctional P2x2/3 heterotrimers by ATP enhances the cholinergic tone in obstructed human urinary bladders. *J. Pharmacol. Exp. Ther.* 372:63–72.

111. Dal Ben, D., M. Buccioni, …, R. Volpini. 2018. Investigation on 2′,3′-*O*-substituted ATP derivatives and analogs as novel P2X3 receptor antagonists. *ACS Med. Chem. Lett.* 10:493–498.

112. Baubichon-Cortay, H., L. G. Baggetto, …, A. Di Pietro. 1994. Overexpression and purification of the carboxyl-terminal nucleotide-binding domain from mouse P-glycoprotein. Strategic location of a tryptophan residue. *J. Biol. Chem.* 269:22983–22989.

113. Guarnieri, M. T., B. S. J. Blagg, and R. Zhao. 2011. A high-throughput TNP-ATP displacement assay for screening inhibitors of ATP-binding in bacterial histidine kinases. *Assay Drug Dev. Technol.* 9:174–183.

114. Rangrez, A. Y., M. Y. Abajy, …, E. Grohmann. 2010. Biochemical characterization of three putative ATPases from a new type IV secretion system of Aeromonas veronii plasmid pAC3249A. *BMC Biochem.* 11:10.

115. Chatterjee, A., S. Singh, …, L. C. Rai. 2020. Functional characterization of Alr0765, A hypothetical protein from *Anabaena* PCC 7120 involved in cellular energy status sensing, iron acquisition and abiotic stress management in *E. coli* using molecular, biochemical and computational approaches. *Curr. Genomics.* 21:295–310.

116. Biswas, E. E., S. B. Biswas, and J. E. Bishop. 1986. The dnaB protein of *Escherichia coli*: mechanism of nucleotide binding, hydrolysis, and modulation by dnaC protein. *Biochemistry.* 25:7368–7374.

117. Plesniak, L., Y. Horiuchi, …, J. A. Adams. 2002. Probing the nucleotide binding domain of the osmoregulator EnvZ using fluorescent nucleotide derivatives. *Biochemistry.* 41:13876–13882.

118. Hellen, E. H., and P. R. Pratap. 1997. Nucleotide binding to IAF-labelled Na+/K(+)-ATPase measured by steady state fluorescence quenching by TNP-ADP. *Biophys. Chem.* 69:107–124.

119. Aguayo-Ortiz, R., and L. M. Espinoza-Fonseca. 2020. Linking biochemical and structural states of SERCA: achievements, challenges, and new opportunities. *Int. J. Mol. Sci.* 21:4146.

120. Clausen, J. D., D. B. McIntosh, …, J. P. Andersen. 2016. Determination of the ATP affinity of the sarcoplasmic reticulum Ca(2+)-ATPase by competitive inhibition of [γ-(32)P]TNP-8N3-ATP photolabeling. *Methods Mol. Biol.* 1377:233–259.

121. Toyoshima, C., S. Iwasawa, …, G. Inesi. 2013. Crystal structures of the calcium pump and sarcolipin in the Mg2+-bound E1 state. *Nature.* 495:260–264.

122. Bublitz, M., L. Kjellerup, …, A.-M. L. Winther. 2018. Tetrahydrocarbazoles are a novel class of potent P-type ATPase inhibitors with antifungal activity. *PLoS One.* 13:e0188620.

123. Saffioti, N. A., M. de Sautu, …, I. C. Mangialavori. 2019. E2P-like states of plasma membrane Ca^{2+}-ATPase characterization of vanadate and fluoride-stabilized phosphoenzyme analogues. *Biochim. Biophys. Acta Biomembr.* 1861:366–379.

124. Hua, S., H. Ma, …, C. Toyoshima. 2002. Functional role of "N" (nucleotide) and "P" (phosphorylation) domain interactions in the sarcoplasmic reticulum (SERCA) ATPase. *Biochemistry.* 41:2264–2272.

125. Bandorowicz-Pikuła, J., and Y. C. Awasthi. 1997. Interaction of annexins IV and VI with ATP. An alternative mechanism by which a cellular function of these calcium- and membrane-binding proteins is regulated. *FEBS Lett.* 409:300–306.

126. Fischer, W., Z. Zadori, …, P. P. Mager. 2007. Conserved lysin and arginin residues in the extracellular loop of P2X(3) receptors are involved in agonist binding. *Eur. J. Pharmacol.* 576:7–17.

127. Kadenbach, B., V. Frank, …, J. Napiwotzki. 1997. Regulation of respiration and energy transduction in cytochrome c oxidase isozymes by allosteric effectors. *Mol. Cell. Biochem.* 174:131–135.

128. Rieger, T., J. Napiwotzki, …, B. Kadenbach. 1995. The number of nucleotide binding sites in cytochrome C oxidase. *Biochem. Biophys. Res. Commun.* 217:34–40.

129. Mou, T. C., A. Gille, …, S. R. Sprang. 2006. Broad specificity of mammalian adenylyl cyclase for interaction with 2′,3′-substituted purine- and pyrimidine nucleotide inhibitors. *Mol. Pharmacol.* 70:878–886.

130. Hiratsuka, T. 1983. New ribose-modified fluorescent analogs of adenine and guanine nucleotides available as substrates for various enzymes. *Biochim. Biophys. Acta.* 742:496–508.

131. Jameson, D. M., and J. F. Eccleston. 1997. Fluorescent nucleotide analogs: synthesis and applications. *Methods Enzymol.* 278:363–390.

132. Bujalowski, W., and M. M. Klonowska. 1993. Negative cooperativity in the binding of nucleotides to *Escherichia coli* replicative helicase DnaB protein. Interactions with fluorescent nucleotide analogs. *Biochemistry.* 32:5888–5900.

133. Jezewska, M. J., A. L. Lucius, and W. Bujalowski. 2005. Binding of six nucleotide cofactors to the hexameric helicase RepA protein of plasmid RSF1010. 2. Base specificity, nucleotide structure, magnesium, and salt effect on the cooperative binding of the cofactors. *Biochemistry.* 44:3877–3890.

134. Virginio, C., G. Robertson, …, R. A. North. 1998. Trinitrophenyl-substituted nucleotides are potent antagonists selective for P2X1, P2X3, and heteromeric P2X2/3 receptors. *Mol. Pharmacol.* 53:969–973.

135. Kasuya, G., T. Yamaura, …, O. Nureki. 2017. Structural insights into the competitive inhibition of the ATP-gated P2X receptor channel. *Nat. Commun.* 8:876.

136. Humphrey, W., A. Dalke, and K. Schulten. 1996. VMD: visual molecular dynamics. *J. Mol. Graph.* 14:33–38, 27–28.

137. Liu, R., and F. J. Sharom. 1997. Fluorescence studies on the nucleotide binding domains of the P-glycoprotein multidrug transporter. *Biochemistry.* 36:2836–2843.

138. Fonin, A. V., A. I. Sulatskaya, …, K. K. Turoverov. 2014. Fluorescence of dyes in solutions with high absorbance. Inner filter effect correction. *PLoS One.* 9:e103878.

139. Sauna, Z. E., and S. V. Ambudkar. 2001. Characterization of the catalytic cycle of ATP hydrolysis by human P-glycoprotein. The two ATP hydrolysis events in a single catalytic cycle are kinetically similar but affect different functional outcomes. *J. Biol. Chem.* 276:11653–11661.

140. Davidson, G. A., and M. C. Berman. 1985. Interaction of valinomycin and monovalent cations with the (Ca2+,Mg2+)-ATPase

of skeletal muscle sarcoplasmic reticulum. *J. Biol. Chem.* 260:7325–7329.

141. Strauss, M. J. 1970. Anionic sigma complexes. *Chem. Rev.* 70:667–712.
142. Hiratsuka, T. 1976. Fluorescence properties of 2′ (or 3′)-O-(2,4,6-trinitrophenyl) adenosine 5′-triphosphate and its use in the study of binding to heavy meromyosin ATPase. *Biochim. Biophys. Acta.* 453:293–297.
143. Chavali, V. R. M., C. Madhurantakam, …, A. K. Ghosh. 2008. Genome segment 6 of Antheraea mylitta cypovirus encodes a structural protein with ATPase activity. *Virology.* 377:7–18.
144. Yao, H., and L. B. Hersh. 2006. Characterization of the binding of the fluorescent ATP analog TNP-ATP to insulysin. *Arch. Biochem. Biophys.* 451:175–181.
145. MacGregor, G. G., K. Dong, …, S. C. Hebert. 2002. Nucleotides and phospholipids compete for binding to the C terminus of KATP channels. *Proc. Natl. Acad. Sci. USA.* 99:2726–2731.
146. Dong, K., L. Tang, …, S. C. Hebert. 2002. Localization of the ATP/phosphatidylinositol 4,5 diphosphate-binding site to a 39-amino acid region of the carboxyl terminus of the ATP-regulated K+ channel Kir1.1. *J. Biol. Chem.* 277:49366–49373.
147. Bandorowicz-Pikula, J., A. Wrzosek, …, S. Pikula. 1997. The relationship between the binding of ATP and calcium to annexin IV. Effect of nucleotide on the calcium-dependent interaction of annexin with phosphatidylserine. *Mol. Membr. Biol.* 14:179–186.
148. Linke, D. 2009. Detergents: an overview. *Methods Enzymol.* 463:603–617.
149. Patel, M. J., S. B. Biswas, and E. E. Biswas-Fiss. 2019. Functional significance of the conserved C-Terminal VFVNFA motif in the retina-specific ABC transporter, ABCA4, and its role in inherited visual disease. *Biochem. Biophys. Res. Commun.* 519:46–52.
150. Ito, K., Y. Murayama, …, H. Iwasaki. 2020. Real-time tracking reveals catalytic roles for the two DNA binding sites of Rad51. *Nat. Commun.* 11:2950.
151. Fraga, J. S., Z. Sárkány, …, S. Macedo-Ribeiro. 2019. Genetic code ambiguity modulates the activity of a C. albicans MAP kinase linked to cell wall remodeling. *Biochim. Biophys. Acta. Proteins Proteom.* 1867:654–661.
152. Li, M., and H. B. Shu. 2020. Dephosphorylation of cGAS by PPP6C impairs its substrate binding activity and innate antiviral response. *Protein Cell.* 11:584–599.
153. Zatopek, K. M., E. Alpaslan, …, A. F. Gardner. 2020. Novel ribonucleotide discrimination in the RNA polymerase-like two-barrel catalytic core of family D DNA polymerases. *Nucleic Acids Res.* 48:12204–12218.
154. Tian, L. F., M. Li, …, S. Mann. 2019. Artificial morphogen-mediated differentiation in synthetic protocells. *Nat. Commun.* 10:3321.
155. Moreau, N. G., N. Martin, …, S. Mann. 2020. Spontaneous membrane-less multi-compartmentalization *via* aqueous two-phase separation in complex coacervate micro-droplets. *Chem. Commun. (Camb.).* 56:12717–12720.
156. Bragança, B., and P. Correia-de-Sá. 2020. Resolving the ionotropic P2X4 receptor mystery points towards a new therapeutic target for cardiovascular diseases. *Int. J. Mol. Sci.* 21:E5005.
157. Obrecht, A. S., N. Urban, …, R. Hausmann. 2019. Identification of aurintricarboxylic acid as a potent allosteric antagonist of P2X1 and P2X3 receptors. *Neuropharmacology.* 158:107749.
158. Merli, A., A. N. Szilágyi, …, M. Vas. 2002. Nucleotide binding to pig muscle 3-phosphoglycerate kinase in the crystal and in solution: relationship between substrate antagonism and interdomain communication. *Biochemistry.* 41:111–119.